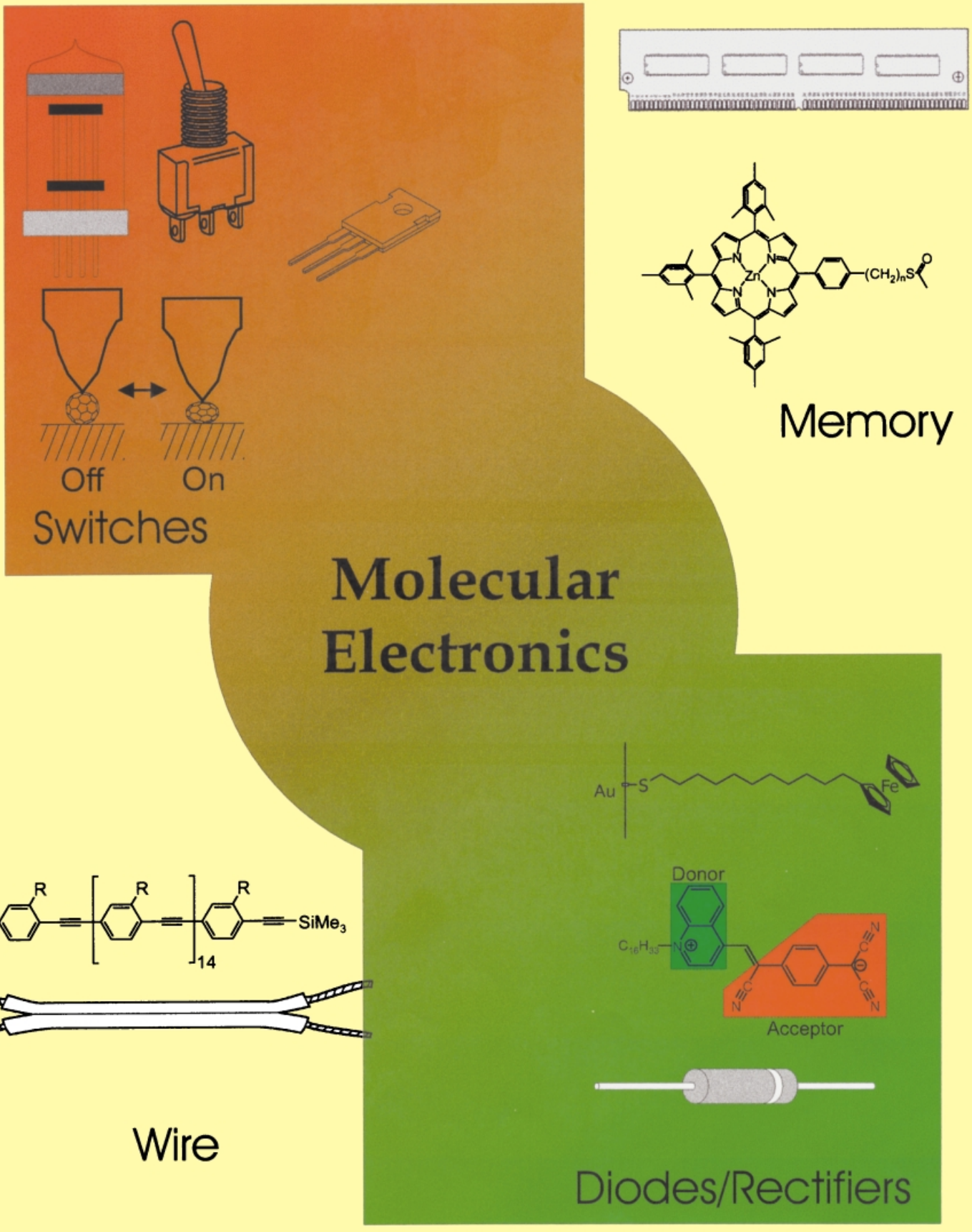

ANGEWANDTE CHEMIE
© WILEY-VCH

The Genesis of Molecular Electronics

R. Lloyd Carroll and Christopher B. Gorman*

Molecular electronics is, relatively speaking, a young field. Even so, there have been many significant advances and a much greater understanding of the types of materials that will be useful in molecular electronics, and their properties. The purpose of this review is to provide a broad basis for understanding the areas where new advances might arise, and to provide introduction to the subdisciplines of molecular electronics. This review is divided into two major parts; an historical examination of the development of conventional electronics, which should provide some understanding of the push towards molecular electronics. The problems associated with continuing to shrink conventional systems are presented, along with references to some of the efforts to solve them. This section is followed by an in-depth look at the most important research into the types of behaviors that molecular systems have been found to display.

Keywords: · molecular electronics · molecular switches · monolayers · scanning-probe techniques

1. Conventional Electronics and Its Boundaries

1.1. Transistor Development and Moore's Law

In the first half of the 20th century, both the study of electronics and the electronics industry grew at a rapid pace. This growth was, in large part, a result of the proliferation of communication devices such as the radio and telephone, and the wartime development of radar. The foremost problem associated with these devices was that of signal amplification. Early efforts used semiconductor crystals as rectifiers to convert an AC signal into DC. However, these systems did not respond well to rapid changes in the signal and were prone to burn-out.

AT&T opened their transcontinental telephone system in 1915. For a telephone signal to travel from one coast to the other, the signal required amplification at several points along the trip. After World War II, it was felt that the system in place, based on vacuum-tube amplifiers called "audions", could be improved by using solid-state devices. In August of 1945, AT&T Bell Labs set up the Solid State Physics group and set them to work to develop a solid-state amplifier.

The first transistor was invented in 1947 by John Bardeen and Walter Brattain at Bell Labs. The point-contact transistor consisted of a slab of germanium in contact with three gold wires (Figure 1). William Shockley followed in 1948 with the invention of the bipolar junction transistor, which controlled current flow through alternating layers of p-type and n-type germanium (Figure 2). Easier to fabricate than the point contact devices, the junction devices were manufactured for many years, with reductions in size and improvements in semiconductor quality. In 1954, germanium was replaced with the development of the silicon transistor at Texas Instruments.

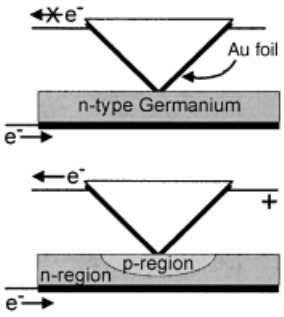

Figure 1. Schematic of a point contact transistor without applied bias (above) and with applied bias (below).

Junction transistors were used in the development of the first integrated circuit in 1958 by Jack Kilby at Texas Instruments (2000 Nobel Prize in Physics),[1] and their use continued until 1961 when they began to be replaced by

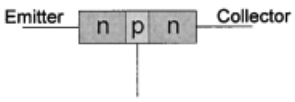

Figure 2. Schematic of bipolar junction transistor.

[*] Prof. C. B. Gorman, Dr. R. L. Carroll
Department of Chemistry
North Carolina State University
Box 8204, Raleigh, NC 27695-8204 (USA)
Fax: (+1) 919-515-8920
E-mail: chris_gorman@ncsu.edu

 © 2002 WILEY-VCH Verlag GmbH & Co. KGaA, Weinheim 1433-7851/02/4123-4379 $ 20.00+.50/0

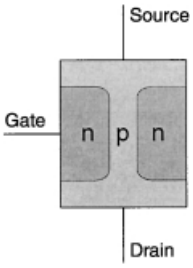

Figure 3. Schematic of field effect transistor.

field-effect transistors (FETs; Figure 3). A FET functions by controlling the migration of electrons or holes into a conduction channel between a source and drain electrode. The amount of migration controls the current through the conduction channel; a large migration (caused by a large signal) can be turned into an even larger current flow between source and drain, thus amplifying the signal.

The integration of complete circuits (including wires, resistors, capacitors, and transistors) on a single piece of silicon was the stimulus for the increase of computational power in the late Fifties. By developing new techniques to fabricate smaller and smaller components, and thus fit more and more components into each cm^2 of silicon, engineers have driven the speed and capabilities of computing at a predictably fast pace. In 1965, Intel co-founder Gordon Moore observed that the number of transistors per cm^2 of silicon doubled every year, and predicted that it would do so for the next 10 years.[2] This statement, or "Moore's Law" as it became known, was revised by Moore in 1975 to state that chip densities would double every 2 years.[3] Looking back, it is now accepted that computational power (which is a convolution of the number of transistors, clock speed, pitch size, and other factors) doubles every 18 months. The predictive power of this statement can be observed on the plot in Figure 4.

Obviously, this reduction in size of components, and thus increase in speed, can only continue for some finite time. Given the current rate of technological advancement, Moore's Law will be accurate for, at most, 20 more years before the components will be reduced to the molecular scale. At this point, and in fact, well before it, current techniques for integrated-circuit fabrication will have been surpassed. New processes will have to be developed, and in fact are in development, in an effort to extend the useful functionality of silicon integrated circuits.

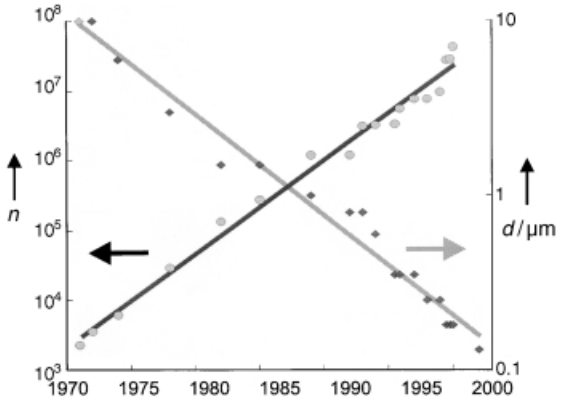

Figure 4. "Moore's Law"—the development of the number of transistors per square centimeter (n) and the pitch size (d) over time.

1.2. Conventional Techniques—Limitations and Outlook

Currently, integrated circuits are made by a photolithographic process, with multiple steps including metal deposition and deposition and doping of silicon to form p-type and n-type silicon. The steps necessary to construct a Junction FET are outlined in Figure 5. There exist several significant challenges in the miniaturization of conventional techniques to prepare integrated circuits. One important limitation in the fabrication process lies in the photolithography step. The wafer, with a layer of photoresist, is exposed through a patterned mask, or reticle. In development, the exposed regions are washed away, leaving the unexposed regions (in positive photoresists), or the exposed regions remain while

Lloyd Carroll received his Ph.D. in chemistry from North Carolina State University in 2001. Prior to that, he taught high school for three years after receiving his BS in secondary education at North Carolina State University. He currently is a postdoctoral research associate in Richard Superfine's laboratory in the Department of Physics at University of North Carolina, Chapel Hill.

Christopher Gorman was born in Summit, New Jersey in 1965. He received his BA in chemistry and computer science from Drew University in 1987 and a Ph.D. in chemistry from the California Institute of Technology in 1991 (with R. H. Grubbs). He then did postdoctoral work with Dr. Seth Marder at the NASA Jet Propulsion Laboratory and with Professor George Whitesides at Harvard University. In 1994, he joined the faculty of North Carolina State University where he is now an associate Professor of chemistry. His present research interests include the design and synthesis of new, polymeric materials with interesting and useful electronic properties at nanometer length scales and the use of scanned probe microscopies in nanoscience to establish molecular structure–property relationships for single-molecule electronic behavior.

R. L. Carroll C. B. Gorman

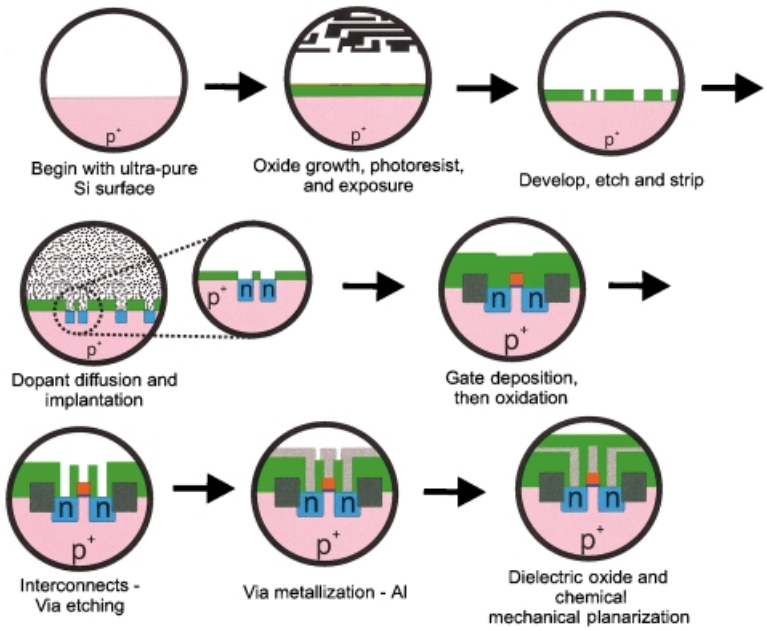

Figure 5. The basic steps to fabricate a Junction FET: an ultra-pure silicon wafer is oxidized, then the oxide patterned by photolithography. The resulting pattern is developed, etched, then any remaining photoresist is stripped. The patterned oxide protects part of the surface during the implantation step, when dopants are added to certain regions of the surface. Using photolithography and chemical vapor deposition, a polysilicon gate is deposited on top of a thin gate oxide. Further layers of oxide are added to separate components and to protect others. Vias are etched through the oxides to allow contact to active regions. Interconnects are deposited—aluminum is evaporated, copper is electrolytically deposited. Further oxides protect one layer from the layer of interconnections above. Finally, the surface is polished by chemical–mechanical polishing to prepare it for the next layer of interconnects and components.

the unexposed regions are washed away (in negative photoresists). The achievable resolution is somewhat dependent on system requirements (both the line resolution d and depth-of-focus D_f requirements), and these obey Equations (1) and (2) where k_1 and k_2 are experimentally determined parameters dependent on the desired critical dimensions, λ the wave length, and NA is numerical aperture.

$$d = \frac{k_1\lambda}{NA} \quad (1)$$

$$D_f = \frac{\pm k_2\lambda}{(NA)^2} \quad (2)$$

It is thus apparent that there are a few ways to improve the resolution of integrated-circuits features. Notably, shorter wavelengths, and larger NAs provide better resolution. There are a number of resolution-enhancing techniques being researched (and already in use) that use longer wavelengths to produce smaller resolution lines than would be immediately attainable, but many of these techniques require greater fabrication time, and thus sacrifice throughput. The most direct means of improving resolution is to move to shorter wavelengths.

Currently, fabrication of state-of-the-art integrated circuits uses 248-nm radiation from a mercury arc lamp (the "I-line") to produce 0.18 and 0.25 μm features, but other fabrication facilities are switching to the use of 248-nm KrF Excimer lasers. Further plans (based on the 2000 International Technology Roadmap for Semiconductors (ITRS)[4]) call for the implementation of 193 nm (ArF Excimer laser) and 157 nm (KrCl Excimer laser) by 2002 and 2005, respectively, to reach the Roadmap goals of 0.13 μm and 0.10 μm pitch. Below 100 nm, there are several options being researched, which include X-Ray lithography ($\lambda < 1$ nm), to attain critical dimensions of down to 70 nm,[5] and extreme UV lithography ($\lambda \approx 13-4.5$ nm), to attain critical dimensions of 70–30 nm.[6] At these wavelengths, there are a number of problems, which include difficulties in focusing the exposing radiation and designing appropriate mask materials and photoresists.

Not only must the pitch of chip features (that is, the distance between parallel features) be minimized, but the depth, or thickness of the features must also scale with width. This requirement is most problematic in the FET-polysilicon-gate region, where in current integrated circuits the gate is insulated by approximately 3 nm of thermally grown oxide from the current channel. To maintain the development path, the oxide layer must continue to shrink. However, it has been shown that once the oxide layer reaches a thickness of < 1.2 nm, it no longer insulates effectively.[7] According to the ITRS, this thickness should be reached by around 2012, and further development of integrated circuits will require the development of new dielectric materials. Current research is focused on metal oxides (notably: Al_2O_3, Ta_2O_5, ZrO_2, and HfO_2) as high-k dielectric gate materials.[8]

As the dimensions of components are reduced, the wiring connecting them must also decrease in size. Such interconnects are currently composed of an Al/Cu alloy, and are insulated from each other by an SiO_2 dielectric. One of the primary problems with such systems is that of electromigration. As current passes through a wire (or interconnect), it has a tendency to transfer some of its momentum to the atoms in the lattice of the metal, particularly at grain boundaries or other defect sites in the lattice. At high current densities (such as those found in the very narrow interconnects), this can, over time, open voids in the interconnect or crack the surrounding dielectric and extrude the metal of the interconnect.[9] In either case, the connection eventually fails. There are many factors that affect electromigration, but the most important is that of temperature. High resistivity in the interconnect (as a result of grain boundaries, defects or poorly oriented grains) can increase resistive heating, which increases the rate of electromigration. Similarly, some of the dielectrics in use to insulate interconnects have very low thermal-conduction properties, and heat generated in the interconnect is not easily removed. Copper is much less susceptible to electromigration,[10] and thus, the use of copper instead of aluminum interconnects should solve several of these problems. However, copper is not as easily processed (at least by current methods) during fabrication. Other effects

that the use of copper introduces are the poor adhesion between copper and the substrate, and the tendency of copper to diffuse into the semiconductor, poisoning it. To solve these new problems, the pre-deposition of a layer, such as titanium or palladium that acts as both a diffusion barrier and adhesion promoter is used.[11] One further limitation that will manifest itself as conventional semiconductor structures grow smaller is that of tunneling. As the distance between device components shrinks, it becomes more likely that current will tunnel between components, rather than conduct along them, introducing errors into computation. The development of low-*k*-value dielectric insulators, such as SiLK,[12] will extend the functional life of conventional integrated circuits. In addition, high-quality lithographic techniques that minimize edge and feature roughness should also minimize unwanted tunneling between closely spaced components.

Even considering further advancements in the science of making integrated circuits, the fact remains that the materials and processes currently in use will reach their fundamental limits sometime in the near future. That eventuality forces us to consider other options. Instead of continuing to make the existing components smaller and smaller, much research is focused towards going directly to the smallest components that are likely to be functional—single molecules and small groups of molecules.

1.3. Definition of Molecular Electronics[13, 14]

Since the size of components in integrated circuits are shrinking in accordance with Moore's law, it is a simple matter to suggest that the ultimate integrated circuits will be constructed at the molecular or atomic level. Such a scenario was suggested in a 1959 lecture by the eminent physicist and visionary, Richard Feynman:

> "I don't know how to do this on a small scale in a practical way, but I do know that computing machines are very large; they fill rooms. Why can't we make them very small, make them of little wires, little elements—and by little, I mean little. For instance, the wires should be 10 or 100 atoms in diameter, and the circuits should be a few thousand angstroms across…there is plenty of room to make them smaller. There is nothing that I can see in the physical laws that says the computer elements cannot be made enormously smaller than they are now. In fact, there may be certain advantages."[15]

At this time, it is impossible to position atom by atom—the capability simply has not been realized. However, what about molecules? Can we control the position of individual molecules or particular groups of molecules such that we can make them do useful tasks? Can we use the electronic properties intrinsic in these molecules to replace larger scale devices? The search for answers to these questions is the field of molecular electronics.

Molecular electronics can be defined as technology utilizing single molecules, small groups of molecules, carbon nanotubes, or nanoscale metallic or semiconductor wires to perform electronic functions.[16] Some have defined it as technologies utilizing only single molecules, but this definition is far too limiting. From the broader definition, it can be suggested that any device utilizing molecular properties is a molecular electronic device. However, in order for a molecular system to be considered a device, there are several requirements that it must meet.

The simplest device that is easily conceived is a switch. The defining characteristic of a switch is that of bistability—it has an "ON" and "OFF" position. Thus, any molecular switch must perform in a similar manner. In its "ON" position, the switch must either perform some function or allow another device to perform its function. In the "OFF" position, it must totally impede the function. Similarly, the switch must not spontaneously change states—it must remain in the position that it is placed until its position is changed. *The development of a molecular switch is perhaps the single most important element in developing molecular replacements for conventional integrated circuits.*

For a molecular switch to be useful, it must be addressable—that is, it must remain in the physical location in space where it is placed, and it must maintain a separate identity from other switches around it. There are two important concerns in this regard. First, it is presently somewhat difficult to position molecules exactly where they are desired. Certainly there are examples of both atomic and single molecular[17] positioning, however, these examples have not been focused at limiting the long-term propensity of the molecule to diffuse. In addition, these previous experiments examined the movement and positioning of mobile molecules on a surface—in a molecule-based system, the molecules must be bound in place (and that they should be in some sort of array) to facilitate addressibility. A primary consideration of any molecular electronic candidate must be that of chemical stability. It is important to understand the long-term stability of any molecular electronics component under a wide variety of conditions. If a molecule tends to decompose when exposed to elevated temperatures, then it is not a good candidate for use in a molecular electronic device. Similarly, the species must be inert with regards to other molecules of the same type, a requirement that is particularly important in devices involving charge-storage or redox-active molecules. Species that show poor "insulation" from each other would tend to exchange stored electrons, scrambling any data represented by the storage of those electrons. Conversely, a molecule which shows an irreversible electron transfer would not be a good candidate for any sort of molecular electronic device as the point of electronics is to utilize reversible charge transfer from one element to the next.

Finally, describing a molecule doing some useful function does not automatically make it a molecular electronic device—there must be a way to interact with the component, both on a microscopic level and through input from the macroscopic world. Thus it is important to consider how a molecular electronic device can be "wired up". It must be able to exchange information, or transfer states to other molecular electronic devices, or it must be able to interface with the components in the system that are not nanoscopic. These requirements present challenges which, as of the date of this review, are just beginning to be addressed.

2. Towards Molecular Devices

2.1. Historical Beginnings—Molecular Rectifiers

The first theoretical and experimental efforts in the molecular electronics arena began in the 1970s with the work of Aviram and Ratner, and their preparation and characterization of donor–acceptor (D–A) species. As is detailed below, some of these results eventually had to be retracted. However, from a historical perspective, they represent an important first attempt to predict and characterize a molecular-scale electronic phenomenon.

By studying an organic analogue of a p–n junction, Aviram and Ratner surmised[18] that such a molecule would act as a molecular rectifier. The computational results from a study of one such D–A molecule **1**, composed of a donor moiety

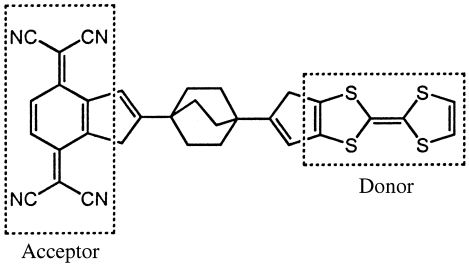

1

tetrathiafulvalene connected by a methylene bridge to an acceptor moiety, tetracyanoquinodimethane, showed a rectification of current should be possible (Figure 6). The rectification behavior can be explained by examining energy-level diagrams for the system (Figure 7). At positive bias (Figure 7b), upon alignment of the metal energy levels with the acceptor LUMO (II), the passage of current begins with the

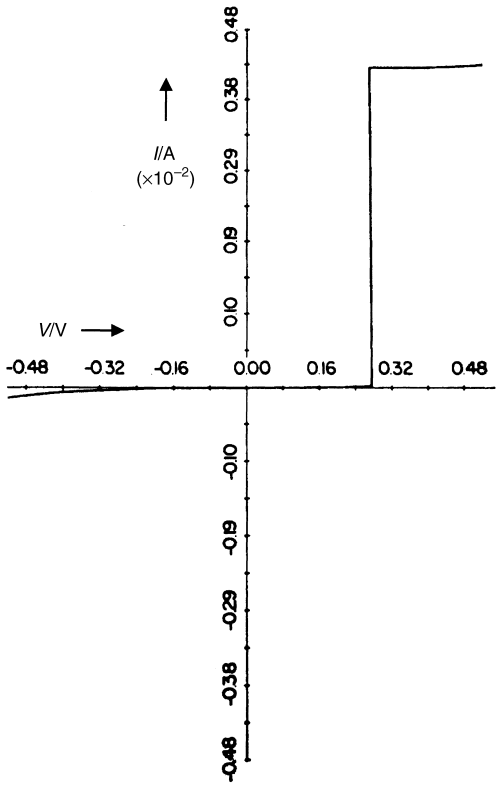

Figure 6. Calculated *I*/*V* Curve for Molecule **1**. Reproduced with permission from ref. [18].

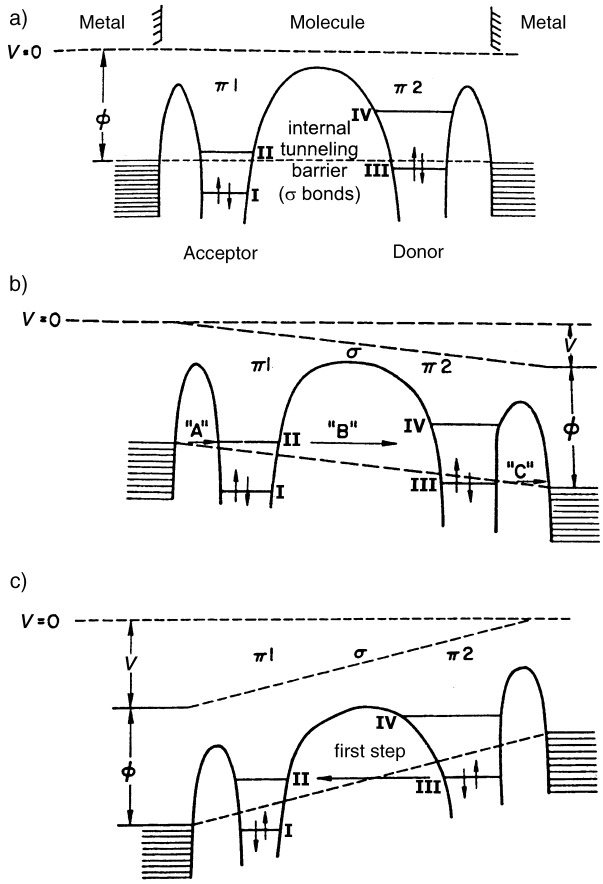

Figure 7. a) Energy-level diagrams of **1**, the donor–acceptor system, between two metal electrodes, b) under positive applied bias c) under reverse applied bias. ϕ = Fermi energy, V = applied bias; modified with permission from ref. [18].

transfer of charge from the cathode to the acceptor (this transfer is represented by "A" in Figure 7b). Charge cannot flow between acceptor and donor, however, until the energy levels of the metal anode are lowered enough to allow charge transfer from the donor HOMO (III) to the metal (this transfer is represented by "C" in Figure 7b). The tunneling process from the acceptor LUMO (II) to the donor HOMO (III) occurs irreversibly ("B" in Figure 7b). Overall, this process has a fairly low threshold voltage, since the molecular energy levels and the metal Fermi energies (E_F) are initially close in energy, and in the proper configuration.

In the reverse bias direction (Figure 7c), there are two mechanisms that must be considered. In one mechanism, similar to that occurring at positive bias, the E_F of the electrode adjacent to the acceptor must be lowered below the acceptor HOMO (I), allowing charge transfer from I to the metal. This allows an electron to tunnel from III to I. The vacancy in III can then be filled by charge transfer from the electrode adjacent to the donor. Another mechanism must also be considered, however, in which the first step is an internal process of tunneling from III to II. Then, charge

transfer can occur from II to the metal, and from the metal to III. Each of these mechanisms requires a substantially larger threshold voltage than at positive bias, and it is this difference in threshold voltage that should give rise to rectifying behavior in such a molecule.

An early effort by Aviram et al. to demonstrate rectifying behavior in a molecule experimentally used a hemiquinone monolayer **2**, the *I*/*V* characteristics of which were probed by

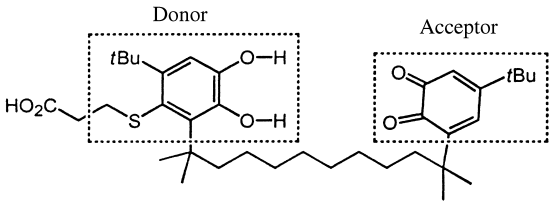

2

an STM tip.[19] In this study, the molecules were immobilized in a self-assembled monolayer on a flat Au surface, the STM-tip motion was stopped and the voltage was varied while monitoring the current. The results seemed to indicate a rectifying behavior in that current flowed very effectively at negative (tip) bias but not at positive bias. It was noted that the catechol moiety in the hemiquinone **2** acts as a donor, while the quinone component is an acceptor. Under negative tip bias (that is, tip negative, surface positive), an electron can flow from the tip to the quinone unit and from the catechol unit to the surface. Proton transfer from the catechol to the quinone unit would very rapidly cancel the dipole, producing semiquinones, which are free-radicals. Since many organic conductors have a partially unfilled HOMO, it was suggested that a semiquinone unit would be a conductor, and thus give enhanced current flow through the molecule. At positive tip bias, the molecular energy levels are unfavorably disposed to carry out this process. Thus, no appreciable current flowed.

As reasonable as the proposed explanation seems, the results were called into question, and eventually retracted[20] when Aviram observed similar behavior in systems lacking these D–A molecules. In addition, there was some evidence that the STM tip was in contact with the surface. These results indicate the experimental difficulties, at least early on, in carrying out these types of studies.

In another attempt to demonstrate rectifying behavior in a molecule, Pomerantz et al.[21] acidified a highly oriented pyrolytic graphite (HOPG) surface, and bound base-substituted copper–phthalocyanine **3** to the modified HOPG.

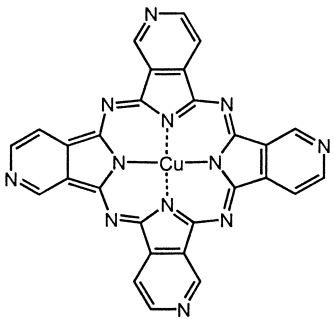

3

Angle-dependent X-ray photoelectron spectroscopy (XPS) indicated that the molecules were bound to the surface at an angle, apparently through one or two of the peripheral amines. The tip was scanned over the surface, and the substrate bias was swept from $+1.2$ V to -1.2 V in less than 100 ms. On clean HOPG, or on HOPG that had been acidified but not exposed to **3**, a relatively symmetric *I*/*V* curve was observed, with a maximum asymmetry ratio $R \leq 2$ as given by Equation (3).

$$R = \frac{|I(-V)|}{|I(+V)|} \tag{3}$$

On HOPG to which **3** had been bound, a large current response was observed at a substrate bias voltage of -1.2 V, with an asymmetry ratio ranging from 10 (over $\approx 60\%$ of the surface) to 40 or more (over $\approx 10\%$ of the surface). These data indicated a strong rectifying effect, presumably because of the presence of **3**. In control experiments, other molecules, specifically, an amine-terminated *n*-alkyl thiol ($HS\text{-}(CH_2)_2\text{-}NH_2$) and a bisquinone-containing amine thiol, were bound to the acidified HOPG and showed *I*/*V* responses identical to the pristine HOPG.

It is apparent that the proposed mechanism for previous systems, based on a donor–acceptor arrangement, is not at work in the HOPG–**3** system. This molecular system has no obvious donor and acceptor. In addition compound **3** is symmetrical, unlike the donor–acceptor systems used in other studies, which have inherent asymmetry in their structure, which gives rise to asymmetry in their *I*/*V* curves.

In an effort to understand the origin of the rectification of current by the bound molecules, UV photoelectron spectroscopy (UPS) was used to determine the density of states (DOS) of the graphite surface both before and after the binding of molecules of **3**. UPS spectra for acidified graphite with and without **3**, and their differences are presented in Figure 8. The difference curve gives the occupied energy

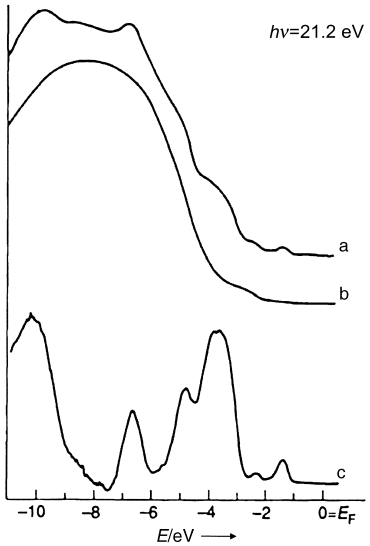

Figure 8. UPS spectra for a) acidified HOPG with bound **3**, b) acidified HOPG (without **3**), c) difference spectrum (a – b). Reproduced with permission from ref. [21].

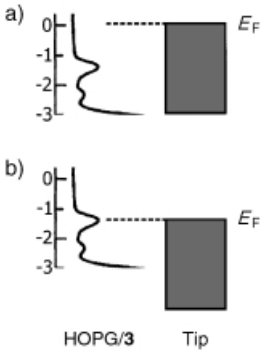

Figure 9. DOS of **3** and HOPG compared to the Fermi energy of the STM tip, at substrate bias of a) 0 V, and b) approximately − 1.3 V.

levels/DOS of **3** below the E_F of the HOPG and shows a maximum at about − 1.3 V. The UPS spectra for the control molecules show no features within several eVs of the E_F. The difference spectrum Figure 9 illustrates that a negative substrate bias of approximately − 1.3 V would bring the Fermi level of the STM-tip into resonance with the feature in the DOS, a requirement for the enhanced tunneling process. Thus, the molecule was responsible for the rectifying behavior present in the system.

Following the work of Martin et al.,[22] Metzger and co-workers[23] have studied Langmuir–Blodgett (LB) films of γ-(*n*-hexadecyl)quinolinium tricyanoquinodimethanide (**4**) between metal electrodes and observed strong rectification behavior. Although compound **4** is a donor–acceptor system,

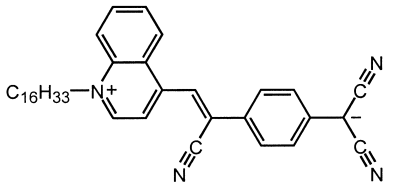

4

it is slightly different from the systems studied by Aviram and Ratner. The major difference is that in **4**, the donor is the quinolinium moiety, connected to the acceptor, tricyanoquinodimethanide by a π bridge. The hexadecyl tail facilitates the formation of LB films (Figure 10). The head-to-tail arrangement was found to be the most stable structure of the LB film. The systems that Aviram and Ratner examined were composed of neutral ground-state donor–acceptor species that became selectively zwitterionic [Eq. (4)].

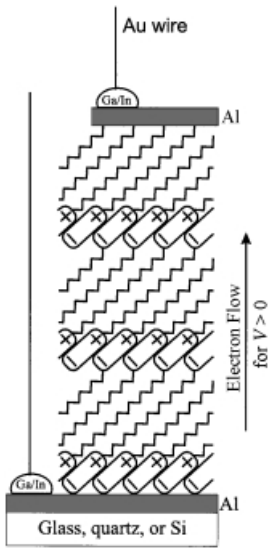

Figure 10. Representation of the LB-film structure of **4** on aluminum. The one and four monolayer films have the same orientation of the molecule.

$$D^+-\sigma-A^- \xleftarrow{1-2\,eV} D-\sigma-A \xrightarrow{9\,eV} D^--\sigma-A^+ \quad (4)$$

The nature of **4**, however, until the work of Metzger et al., was unclear. It was proposed that the ground state was a mixture of zwitterionic and neutral molecules, and that intramolecular electron transfer gave rise to the rectification. Metzger et al. made LB films of **4** on aluminum coated quartz, then with the film at 77 K added a second Al layer on top by evaporation (Figure 10). Connections to the metal pads were made with Ga/In eutectic or an Ag paste. Electrical measurements showed strong rectification. Figure 11 shows the *I*/*V* curves from two different experiments using **4**. In one, a single monolayer of **4** was sandwiched between two Al electrodes. The rectification ratio (RR—identical to the "asymmetric ratio" of Aviram and Ratner) for this sample was about 40. In an analogous experiment, a four-layer-thick LB film was measured with Al electrodes and gave an RR value of more than 10 (Figure 11b).

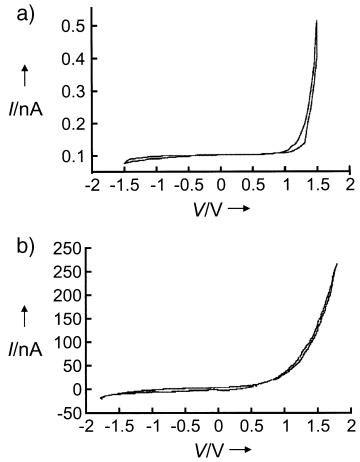

Figure 11. *I*/*V* curves from two different LB-film configurations. a) Ga/In eutectic | Al(100nm) | 1 LB monolayer | Al(100nm) | Ga/In eutectic. b) Ga/In eutectic | Al(100nm) | 4 LB monolayers | Al(100nm) | Ga/In eutectic. Reproduced with permission from ref. [23].

Upon consideration of the LB film structure (Figure 10), a mechanism for the rectifying behavior can be proposed. In the Aviram–Ratner model, electron transfer to/from metal electrodes to a neutral ground-state molecule (Figure 12a, forward bias) creates a zwitterionic form that by intervalence transfer (IVT) can regenerate the neutral form. The overall electron transfer is from acceptor towards donor. If the

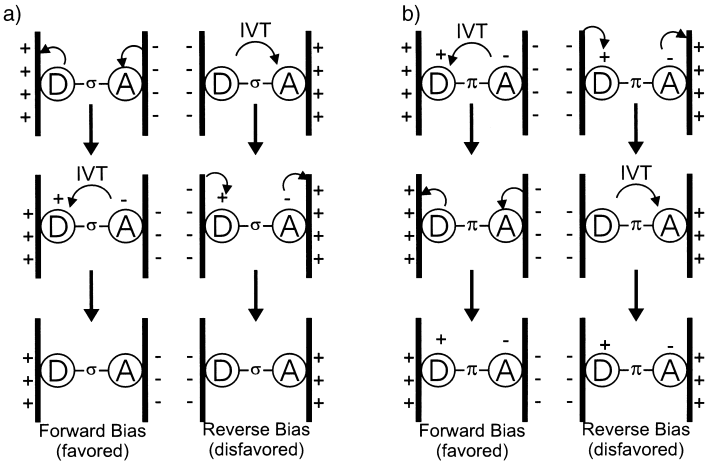

Figure 12. a) Aviram-Ratner model for neutral D-σ-A species, and b) modified model for zwitterionic D^+-π-A^- species.

process is initiated in a zwitterionic molecule (such as **4**), under forward bias the IVT occurs first, creating a neutral molecule (Figure 12b, forward bias), followed by electron transfer to and from the metal to recover the zwitterionic form. As before, this process results in overall electron transfer from acceptor towards donor. The difference in the magnitude of the I/V responses between one and four LB layers (Figure 11a, b) is not entirely clear, but it has been suggested that the larger current flow in the thicker layer results from conduction through defects.[24]

2.2. Wiring Up—Molecular Wires

One of the requirements to using any molecular electronic component is the ability to wire it into a device architecture. To connect molecules to one another, or to the macroscopic world, molecular-scale wires are necessary. In an effort to understand the important characteristics of such a molecular wire, most research in this area has concentrated on linear, conjugated oligomers.

Conjugated oligomers are proconductors.[25, 26] A conductor can be derived from this type of proconductor by either an oxidation or a reduction. In the bulk, polythiophene is a poor conductor, upon oxidation it becomes polythiophenium, a cation, and a much better conductor by virtue of the unfilled HOMO and a change in geometry to create mid-gap states (Figure 13). One can rationalize the relative conductance of

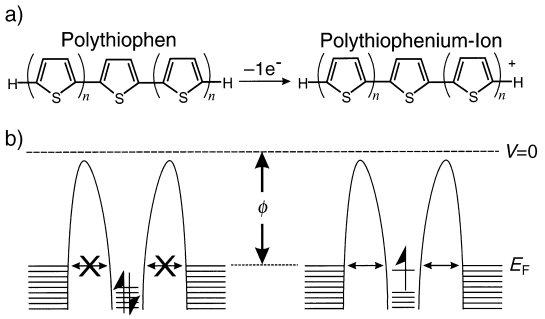

Figure 13. a) Conversion of proconductor (polythiophene) into conductor (polythiophenium) by oxidation, b) simplified energy-level diagrams for the proconductor (left) and conductor (right) between two metal electrodes.

thiophene oligomers in an analogous fashion. Conductor and proconductor pairs may find usefulness in molecular electronics, however, the need to oxidize or reduce them, or introduce a dopant into the bulk makes them less than ideal. Recent work into metal-containing carbon chains and porphyrinic arrays has provided a possible route around these potential limitations.

Gladysz and co-workers[27] have synthesized metal-terminated carbon chains similar to **5**, with up to ten alkynyl units ($Re(C{\equiv}C)_nRe$, $n \leq 10$). Cyclic voltammograms (CV) of three of these molecules are shown in Figure 14a. For the shorter $Re(C{\equiv}C)_2Re$, two single-electron oxidations are observed. For the longer chains ($Re(C{\equiv}C)_3Re$ and $Re(C{\equiv}C)_4Re$), the oxidation becomes increasingly irreversible. The solution cyclic-voltammetry results for the entire family of complexes from $n = 2$ through 10 are shown in Figure 14b. The presence of only a single, presumably two-electron oxidation wave in $Re(C{\equiv}C)_{10}Re$ indicates that once the chain reaches this length, the metals are effectively isolated from one another and do not communicate by the conjugated bridge. These molecules have not been studied under electrode-bound device conditions. However, these results indicate that such a molecule will not be expected to function as an ideal molecular wire.

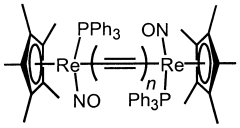

5

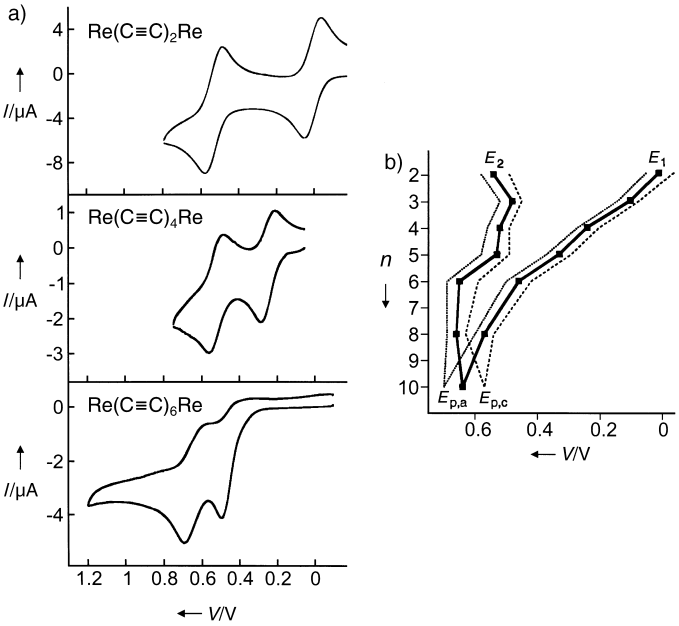

Figure 14. a) Cyclic voltamograms of **5** (10^{-5} M in 0.1M Bu_4N^+ BF_4^-/CH_2Cl_2, Pt working and counter electrodes, potential versus Ag-wire pseudoreference, scan rate = 100 mV s^{-1}, ferrocene = 0.46 V). b) Plot of cyclic voltammetry results for series from $Re(C{\equiv}C)_2Re$ to $Re(C{\equiv}C)_{10}Re$, E_1 is first oxidation, E_2 is second oxidation, $E_{p,c}$ and $E_{p,a}$ are cathodic and anodic peak potentials, respectively. Reproduced with permission from ref. [27].

Potential molecular wires composed of fused porphyrin rings have also been constructed, for example, Crossley and Burn synthesized oligomeric linear porphyrin arrays, such as **6**.[28, 29] Over 100 such systems (e.g., **7**) have been studied

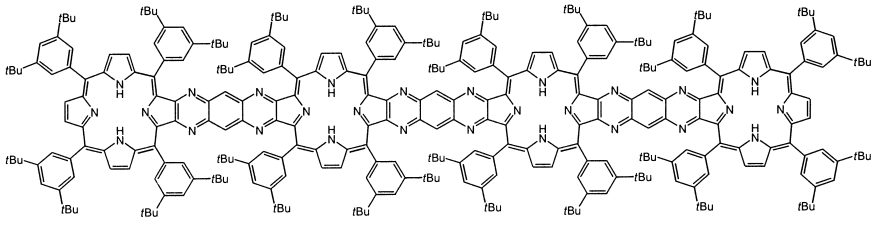

6

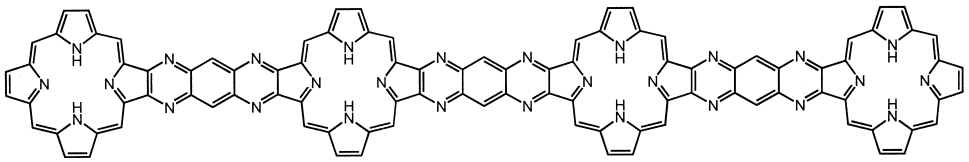

7

computationally[30] in an effort to gauge their potential as molecular wires. These results suggest that the molecular-wire characteristics of these fused ring porphyrins are highly tunable, depending on the substitution of the porphyrin ring, the nature of the bridging unit (1,4,5,8-tetra-azaanthracene in **6** and **7**), and the metal (or lack thereof) in the system. They suggest that the electronic properties of these systems (and presumably others) are dominated by the degree of π delocalization. In π systems of discrete single and double bonds the electrons are more locked in place (localized) than those in which the formal single and double bonds are similar in length. Concomitantly, in nonconjugated systems there is less electronic communication from one end of the molecule to the other. Highly delocalized systems, however, support long-distance communication between parts of the molecule, and thus are desirable in molecular wires. This computational work has laid significant groundwork for understanding the experimental behavior of such molecules.

A large body of experimental work has emerged regarding the electronic behavior of oligo(phenylene ethynylene)s. Tour and co-workers have synthesized many of these types of molecules, the longest is **8** with a length of 128 Å.[31, 32] While the conductivity of this particular molecule has not been determined, a number of significant experiments have been performed on similar shorter molecules to measure their effectiveness as molecular wires.

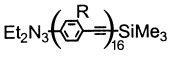

8

Bumm et al.[33, 34] used the tip of an STM to measure the conductivity of single molecular-wire molecules of **9** embedded in a self-assembled monolayer (SAM) support composed

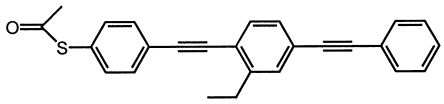

9

of dodecanethiolate (DT). When the thioacetate group on **9** was deprotected to the thiol (**9′**—Figure 15a) in the presence of the crystalline SAM, single molecules, or at most a few molecules, were bound to the underlying Au(111) surface at disordered defects in the SAM. STM imaging revealed bright, stable, isolated spots at domain boundaries and defect sites in the DT SAM (Figure 15b). These bright spots were consistent in size, shape, and orientation, which indicates that they were features sharper than the tip used to image them. In addition, Bumm et al. measured the apparent tunneling-barrier height (ATBH) over DT–**9′**. The ATBH, a measurement of the relative conductivity of the underlying film, may be determined by modulating the position of the STM tip (z) and observing the change in the current (I) with respect to the position (dI/dz). There are many convoluting factors, such as mechanical distortion of the film or tip, in determining a quantitative measure of ATBH.

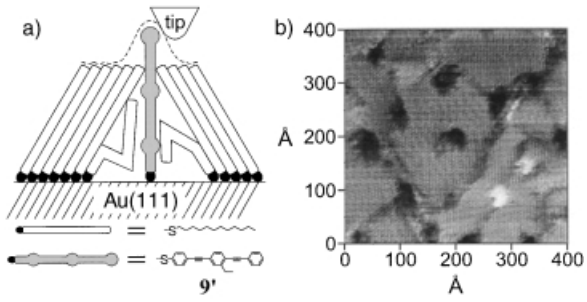

Figure 15. a) Schematic illustration of the insertion of **9′** into a disordered domain boundary of a DT SAM. The dashed line represents the feature as imaged by the STM tip, b) STM image of the arrangement illustrated in (a); the bright spots of similar shape and size are the molecules of **9′**. Figure 15b modified with permission from ref. [33].

By comparing the ATBH over DT with that over **9′**, these factors could be ignored to obtain a relative measure of conductivity. The ATBH over **9′** was observed to be at least two times higher than over DT. The bright spots in Figure 15b indicate the tip withdrawing from the surface, and thus increasing the tip-substrate separation. Considering that the tip is farther away from the substrate, and the ATBH is larger, it was inferred that molecules of **9′** have a greater conductivity than molecules of DT.

These results suggest that oligo(phenylene ethynylene)-type molecules might make good molecular wires. However, some of the results of experiments performed by Myrick's group[35] suggest that this may not be the case. SAMs of **10** (a dithiol similar to **9′**) on Au electrodes were found to passivate

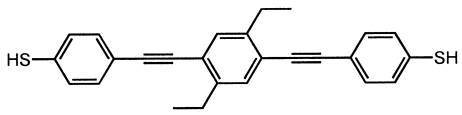

10

the Au electrode in a manner similar to DT-SAMs (Figure 16). Anodic stripping voltammetry (ASV) showed that deposition of Cu occurred at high negative potentials on both DT and **10**. This process happens on bare Au surfaces at about −0.1 V. Copper ions required a significant overpotential to be reduced at defect sites in a DT SAM,[36] and the same effect was observed in SAMs of **10**. Although the relative ease of nucleation of copper metal islands on the SAM of **10** can not be ignored when ascribing reasons for the observed overpotential, the significant shift in potential still suggests that SAMs of **10** are poor electrical conductors.

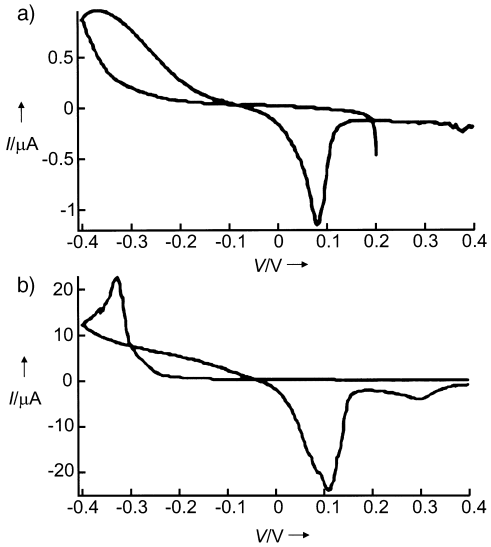

Figure 16. Anodic stripping voltammetry (ASV) of copper on a) Au electrode with a DT SAM b) Au electrode with a SAM of **10**. Reproduced with permission from ref. [35].

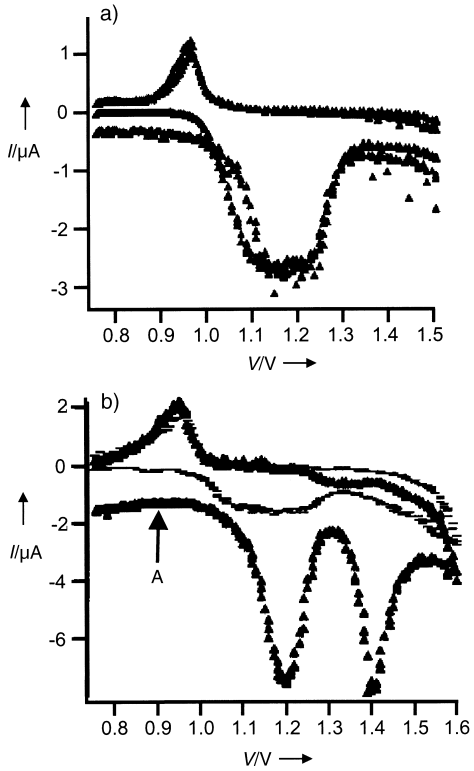

Figure 17. ASV of vapor-deposited Cu on a) a DT SAM, and b) a SAM of **10**. ▲ first scan, – second scan. "A" indicates the position at which potential sweep was stopped and the sample imaged by SEM. Reproduced with permission from ref. [35].

The poor relative conductivity of SAMs of **10** was further suggested in the following experiment. Copper was vapor deposited onto the SAM in an attempt to ensure that a layer of Cu was present atop the defect-free portions of the SAM. Stripping voltammetry on SAMs of both DT and **10** revealed the characteristic stripping peak for copper at +0.1 V. In the DT system also showed a broad peak at +1.2 V indicative of gold oxidation, and the corresponding stripping peak for the oxide at +0.9 V (Figure 17a). A SAM composed of **10** also showed a peak at +1.2 V, but the peak was much sharper than that observed for the DT SAM (Figure 17b). A second sweep on the SAM of **10** revealed the Au oxidation peak that was hidden beneath this sharper peak. The SAM of **10** also showed a peak at +1.4 V that was assigned as the oxidation (and subsequent desorption) of the **10** molecule. The nature of the sharper peak at +1.2 V was made clear when the surface was examined by SEM. When the Cu-covered SAM of **10** was swept to +0.9 V (point A in Figure 17b) then removed from the electrochemical cell, SEM images revealed the presence of Cu islands on top of the SAM of **10**. SEM images of the SAM after sweeping past the +1.2 V sharp peak showed that the islands were gone. Thus the initial sharp peak at +1.2 V on the **10** SAM arises from the stripping of the Cu islands that were on defect-free, ordered domains of the **10** SAM.

The large overpotential (1.1 V) across the molecule (25.2 Å) indicates an electric field strength of about 450 MV m^{-1}, which suggests a tunneling mechanism and therefore, a tunneling barrier. Charge tunneling through a SAM of **10** can occur with holes or electrons as charge carriers. Holes must tunnel through a barrier the height of which is determined by the difference between the Au Fermi energy and the HOMO of the SAM of **10**. The barrier height for electron tunneling is the difference between the Cu Fermi energy and the LUMO of the SAM of **10**. Whichever barrier height is lower will dictate the dominant charge carrier in the molecule. The barrier height can be estimated from the overpotential. Thus, an overpotential of 1.1 V is a crude measure of a barrier height of 1.1 V. The formal oxidation of **10** occurred at +1.4 V, very near to the copper stripping peak at +1.2 V, which suggests that the dominant charge carriers are holes injected from the gold electrode into the HOMO of **10**. Further estimates of the barrier height by independent methods corroborated the value of 1.1 V. The authors concluded that a barrier height of 1.1 V is unsuitable for a molecule intended as a conductor. While at odds with predictions that such a molecule should be a good conductor, the authors concede that there are likely to be differences in the electrical environment of the molecule when probed by a sharp STM tip than with a planar Cu contact.

In any effort to describe a molecular wire, perhaps the most important characteristic is the conductivity of the wire. In other words, how effectively, both in time and distance, is charge transferred from one end of the molecule to the other? An ideal molecular wire would transfer charge over long distances at very fast rates. These are issues that are dealt with at great length in the field of electron transfer.[37] Most molecular entities appear to transfer charge through a tunneling mechanism where the rate of electron transfer shows an exponential dependence on distance. Determining the distance dependence of electron transfer allows comparison of the conductivity of different molecules, regardless of their length. This distance dependence may be represented by an experimentally determined value β, determined from the slope of a plot of $\ln(k_0)$ against distance. Several conjugated oligomer systems have been studied as potential molecular-wire systems, and their β values are presented in Table 1.

Particularly for *n*-alkane chains, β values (for single-electron transfers) have been correlated with the relative conductivity of single-molecule-thick junctions (Majda et al.[38, 39] and by Rampi and Whitesides et al.[40–42] by using metal | molecule | mercury-drop junctions and by Frisbie and Wold[43] using

Table 1. Exponential decay constants β for various molecular repeat units.

Repeat unit	β_{calcd} [Å^{-1}]	β_{exp} [Å^{-1}]	Ref.
oligophenylenevinylene[a]		0.06	[46]
oligophenylethynyl		0.36	[110]
oligoporphyrin **6**	0.045		[111]
polyene	0.078		[112]
alkyl		0.85	[113]

[a] One to four repeat units.

conducting atomic force microscopy). These efforts do not overcome all of the device-related challenges of attaching molecular wires between molecular components, but they do indicate relevant behaviors of different molecular wires.

Using β values to assess the behavior of molecular wires has several important limitations. The exponential distance dependence of electron transfer indicates a single, non-adiabatic transfer using a superexchange (tunneling) mechanism. Recently, systems that show little rate dependence with distance have been illustrated. Davis et al. showed that there is only a weak distance dependence when the energy of donors and acceptors are matched to that of an oligo-phenylene vinylene bridge.[44] While this type of behavior has yet to be observed in a molecular device, the importance of binding between molecule and electrode has been appreciated.[45] Transition from a non-adiabatic to an adiabatic mechanism, which would have consequences for the distance dependence of electron-transfer rates,[47] may have recently been observed in ferrocene-terminated oligophenylene vinylene SAMs on gold.[46] Conformational changes can stimulate a transition from superexchange-mediated electron transfer to thermally activated (hopping) transport.[48, 49] This latter mode has a weak distance dependence and has been proposed to explain the electron-transfer behavior of DNA.[50–54] Arguably, systems with a small or non-existent distance dependence on rate are much better candidates for molecular-wires.

Carbon nanotubes represent another emerging area of interest for molecular scale wires. In recent years, synthesis of single-wall nanotubes (SWNT) has improved dramatically,[55, 56] increasing the amounts of material available and aiding efforts to investigate their properties. It was predicted that the electrical properties of SWNTs should vary depending on their specific chirality and diameter,[57, 58] and scanning probe techniques have been successfully used to verify this by correlating structure with density-of-states.[59, 60]

Generally it has been observed that the largest resistance in a nanotube wire arises from the contact resistance between an electrode and the nanotube. Bachtold et al.[61] studied multi-walled nanotubes in a four-probe configuration and found the contact resistance to be as high as 1 GΩ, while the resistivity of the tube could be as low as 0.3 $\Omega\,\mu m^{-1}$. They modified the contact resistance to around 60 kΩ by scanning the nanotube–electrode junction with the SEM beam, apparently "soldering" the tube to the electrode with the ubiquitous amorphous carbon contaminant.

de Pablo and co-workers[62, 63] used scanning force microscopy to characterize single-wall nanotubes onto which electrodes had been lithographically patterned. They found a contact resistance of 44 kΩ and a tube resistivity of 0.15$\Omega\,\mu m^{-1}$. These results suggest that carbon nanotubes will make very efficient wires in nanoscale systems, if they can be connected well.

There are additionally several significant challenges remaining for the use on carbon nanotubes in molecular electronics. First, there is, as yet, no technique to produce only one type of tube, either metallic or semiconducting. This may not matter given the nature of the examples above. In neither case is the chirality of the tube controllable. Further, there is not yet a reasonable method of separating the different types of tubes produced by current synthetic techniques. Avouris and co-workers have selectively oxidized metallic single-wall nanotubes in bundles with semiconducting nanotubes, so that only semiconducting nanotubes are left. This method may provide a potential route to utilization of only one type of tube in an electrical circuit.[114] Finally, the nanotubes must be explicitly positioned and connected, which is limited currently to serial techniques (electron-beam lithography, scanned probe manipulation). Other techniques are under development (fluid alignment, dielectrophoretic alignment, self-assembly) which will probably improve the outlook for nanotube wires.

Semiconductor nanowires have also emerged as a set of materials with potentially very high utility in molecular electronics. As of the date of this review, this field is moving rapidly—several-hundred papers describing their synthesis and properties have appeared in just the last two years. Some significant efforts are highlighted here—this discussion is far from comprehensive. Advances have been reported for the efficient synthesis of semiconductor nanowires including materials containing segments of different materials along their length.[64–66] This latter type of material builds the equivalent of semiconductor junctions into the nanowire, a potential route into junction-based devices. Polarized luminescence and lasing action has been illustrated in single nanowires.[67–70] Well defined laser sources of nanometer size open up the possibility of photonic information processing at the nanometer scale. The binding of molecules to nanowires influences their electronic properties—this behavior can be the basis of novel, nanoscale sensors (perhaps even for single-molecule detection).[71, 72] By crossing nanowires, multi-terminal junction devices have been fabricated that are capable of logic operations.[73–75] Large-scale integration of crossed nanowires has not yet been achieved. However, several examples have been illustrated in which superlattice structures[76–78] have been prepared using flow techniques.

2.3. Static Elements: Data Storage

In contrast to the dynamic nature of a molecular wire, with its ability to transfer charge from one location to another, a memory device represents a static component. In the current

computational architecture, data is stored in a bit-wise manner—the smallest part of data is either 0 or 1. In a molecular system, there are a number of ways this might be realized, which include charge storage, conformational or positional shifting, and physical transformation.

Nanotubes and their cousins, the fullerenes, have been exploited in the design of prototype nanoscale memories. Lieber's group[79] has proposed a nonvolatile random access memory (RAM) based on a suspended crossbar array of nanotubes (Figure 18). The authors presented calculations

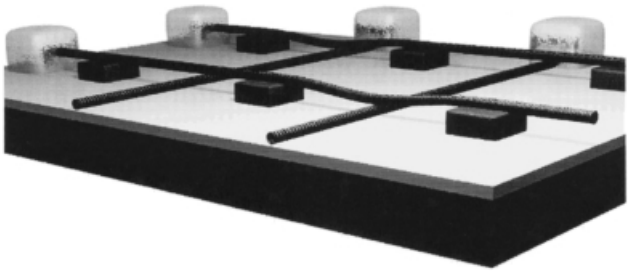

Figure 18. Suspended crossbar configuration of the nonvolatile RAM proposed by Lieber et al. The Figure shows a 3D view of four junctions in the proposed architecture, with two crossbar devices in the ON state (in contact) and two in the OFF state (separated). The upper nanotubes are supported on organic or inorganic supports (black blocks), while the lower nanotubes are directly in contact with insulating substrate (SiO_2, white) on conducting layer (highly doped Si, black). The light gray blocks represent the electrodes used to address each nanotube. Reproduced with permission from ref. [79].

that suggest that, for nanotubes in relatively close proximity to one another, there are two energy minima corresponding to the nanotubes remaining either suspended (OFF) or in contact (ON). The ON state persists as a result of van der Waals interactions between the two nanotubes, and may be initiated in a separated pair by applying voltage pulses of *opposite* polarity to the two crossed nanotubes. The ON state may be switched to the OFF state by applying a larger voltage pulse of *identical* polarity to each of the nanotubes. The device elements may be as small as 5 nm, giving a density of 10^{12} devices per cm^2. The switching time was calculated to be on the order of 10^{-11} s, which gives an operating frequency of approximately 100 GHz.

The theoretical work was supported by experimental measurement of a suspended nanotube junction. The junction was fabricated by mechanical manipulation of the nanotubes and the evaporation of contact electrodes onto them. The device could be switched ON and OFF with applied voltage pulses. The state of the device could be read by measuring the resistance of the junction—the resistance in the OFF state was greater by up to five orders of magnitude than the ON state. The reading of the device should be non-destructive, and thus the junction represents a nonvolatile memory element. Lieber et al. proposed the fabrication of large arrays of such junctions by either patterned growth of the nanotubes in an array, or directed self-assembly, both of which have been demonstrated in different systems.

Kwon and co-workers[80] have proposed the use of so-called "bucky-shuttles" as nonvolatile memory elements. A bucky-shuttle consists of a fullerene (a "buckyball") with a diameter close to that of C_{60} encapsulated inside a short nanotube. These objects were made in abundance from the treatment of nanodiamond powder at 1800 °C. The buckyball was observed to stay at one end or the other of the nanotube, presumably because of van der Waals interactions and weak covalent forces, as has been observed in crystalline C_{60} and nanotube bundles.[55] Calculations of the potential energy of a C_{60} as it shuttles inside a C_{240} shell show a 0.24 eV stabilization at the ends of the shell, compared to anywhere along the length. Reading and writing such a structure necessitates that the fullerene is charged. It was proposed to accomplish this with $K@C_{60}^+$, one of a family of known fullerenes with a caged metal ion. The metal ion within the C_{60} imparts a net positive charge that is evenly distributed over the whole fullerene. Writing of data would occur when a field is applied along the axis of the shell through integrated electrodes in the ends of the shell. A bias of about 1.5 V was calculated to be enough to destabilize one of the energy minima, causing the $K@C_{60}^+$ to migrate to the other end of the tube in around 4 ps. The state of the device can be read nondestructively by measuring the polarity of the capsule, or destructively by applying a probe voltage and measuring the resulting current pulse.

Kwon et al. envisioned arrays of these capsules packed side by side, with crossing electrodes connected to their ends (Figure 19). Individual element addressing is carried out by

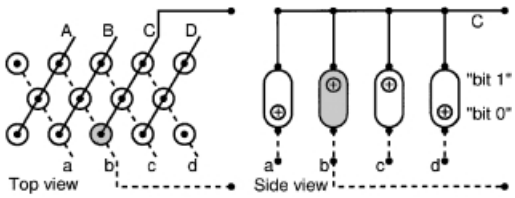

Figure 19. Configuration of "bucky-shuttle" memory elements. left: Top view showing an array of bucky-shuttles and the crossed electrodes used to address them. Right: side view showing the elements addressed by electrode C. By applying a reading or writing pulse between electrodes C and b, a specific element may be queried or written. Reproduced with permission from ref. [80].

applying read or write pulses to crossed electrodes, thereby reading from or writing to the element between them. Under ideal conditions, such an element may be switched at a rate of 100 GHz. The authors did not suggest any method by which an array of closely packed, vertically oriented nanotube-based memory elements might be produced, and thus did not present any predictions on element density.

Other examples of data-storage proposals involve the modification of polymeric materials. While such examples of data storage are not truly molecular electronics, they bear consideration in the context of discussing the current state of the field. Binnig et al.[81] studied the use of thermomechanical techniques to write data into soft polymers. This was accomplished by using a modified cantilever in which the tip was heated by applying a voltage across the legs of the cantilever. Placing this heated cantilever in contact with a polymer layer melted a small region of the surface, forming a pit. Each pit represents a bit of data. It was observed in

previous efforts that using a thick polymer layer led to larger pit sizes and reduced lifetime for the reading/writing tip. This technique has been refined through many iterations to employ multilayer polymer surfaces. The described work of Binning et al. uses a dual-layer substrate composed of 40 nm of polymethylmethacrylate (PMMA) on 70 nm of photoresist baked onto Si. The PMMA is the actual medium of data storage, while the photoresist serves as a physical buffer between the tip and the underlying Si surface.

The actual writing of data into the PMMA layer was accomplished by applying short (2 μs) voltage pulses to the thermomechanical cantilever. This heated the cantilever tip to approximately 400 °C, melting the PMMA and forming a pit. The reading of data employed the writing tip in a constantly heated (≈350 °C) mode. The resistance across the legs of the cantilever shifted linearly with changes in temperature. The temperature of the tip depended on how effectively heat was transferred through the air between tip and substrate or through the legs of the cantilever. When the tip was outside of a pit, the heat transfer was dominated by the cantilever legs, and the tip reached a stable temperature. When the tip moved into a pit, the heat transfer through air became more efficient than through the cantilever legs, and the tip temperature (and resistance) fell. By monitoring the resistance as the tip was scanned over the surface, the presence of pits in the substrate was detected. Erasure of data was accomplished in a similar manner—heating the entire substrate above 150 °C for a moment erased the presence of pits. Multiple writing and erasing cycles were carried out with no degradation of the substrate. Recently, Lutwyche et al.[82] furthered this technique by utilizing an array of 32 × 32 thermomechanical tips to working in a parallel fashion to write data in bit densities as high as 100–200 Gbit per square inch. Improvements in the read and write rates of the parallel array have moved the device closer to production, with a prototype device called "Millipede".[83]

Roth et al.[84] suggested that data may be stored in the oxidation states of molecules, specifically, metalloporphyrins such as **11**. The family of molecules all exhibit reversible one- and two-electron oxidation to the mono- or dication radical. It was suggested that the neutral molecule might represent a bit state of "00", while the monocation represents state "01", and the dication, state "10". To demonstrate the effectiveness of charge storage in the molecule, a SAM of **11a** was prepared on a microelectrode and studied by open-circuit potential (OCP) amperometry. In this electrochemical technique, the molecules in the SAM were oxidized (and data "stored") by a potential step to +800 mV for the monocation ("01"

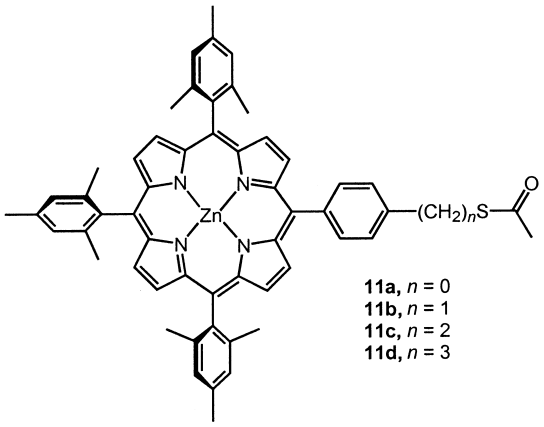

state) or +1100 mV for the dication ("10" state). The counter-electrode (CE) was then disconnected for some time to allow for the dissipation of charge from the electrochemical double-layer. To "read" the data, the CE was then reconnected at the open-circuit potential, which is normally negative enough to reduce the oxidized porphyrin. The current measured is proportional to the oxidation state of the molecules (or their bit state) and the number of molecules in that state (Figure 20). The response time of the measurement was limited by the RC (where R is the total effective resistance of the cell and C is the capacitance of the cell) time constant of the cell. Thus, shrinking the active area of the electrode increased the instantaneous current from the SAM (Figure 20c). In addition, the length of the methylene spacer between the

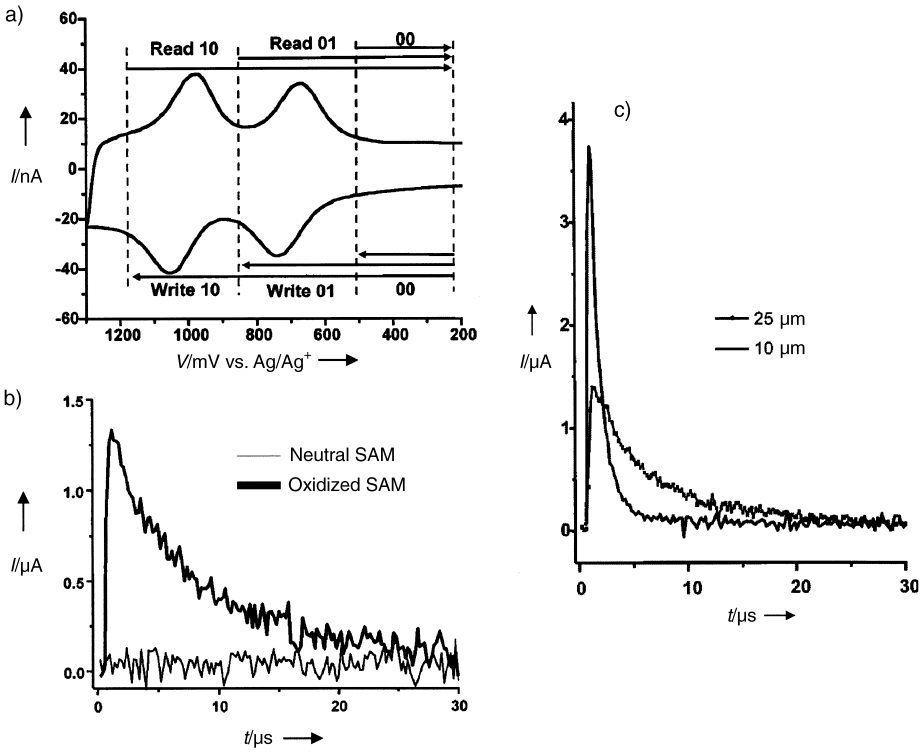

Figure 20. a) CV of **11a** (25 μm diameter Au electrode, in electrolyte solution of 0.1 M $Bu_4N^+PF_6^-$ in dried, distilled CH_2Cl_2 with Ag-wire counter electrode), b) current trace for reconnection of the counter electrode at OCP for neutral and oxidized **11b** SAMs, c) current trace for two Au electrodes (diameter: 25 and 10 μm) with **11b** SAMs, oxidized at +800 mV (versus Ag/Ag^+), disconnected for several seconds, then reconnected at the OCP (+125 mV versus Ag/Ag^+). Reproduced with permission from ref. [84].

porphyrin and the thioacetate was found to have a direct effect on the retention time of the charge storage, based on a determination of decay half life ($t_{1/2} = 116$, 167, 656, and 885 s for **11a–d**, respectively).

2.4. Transistorized: Molecular Switches

The switch is the basic element of control in any electronic architecture—by its very function it either allows current to flow or not. There are many examples of proposed molecular and atomic switches, which use a myriad of different mechanisms and motifs for operation.[85] Aside from "simple" switches there have also been several significant suggestions of more complex switching behaviors, which include the use of arrays of switches to implement logic operations and the use of two-terminal resonant tunneling devices to do the job of switching. A number of examples of molecular switching have been proposed based on quantum effects; single molecules, carbon nanotubes, and quantum dots or nanoparticles have all been found, under the right circumstances, to display some of these quantum effects.

Dekker and co-workers[86] fabricated a field-effect transistor based on a carbon nanotube, and demonstrated weak gain under room temperature conditions. The device consisted of a semiconducting tube positioned across two Pt electrodes, on a SiO_2 substrate, with doped Si as the back gate (Figure 21). The electronic characteristics of the device were measured by sweeping the bias between the two electrodes at various

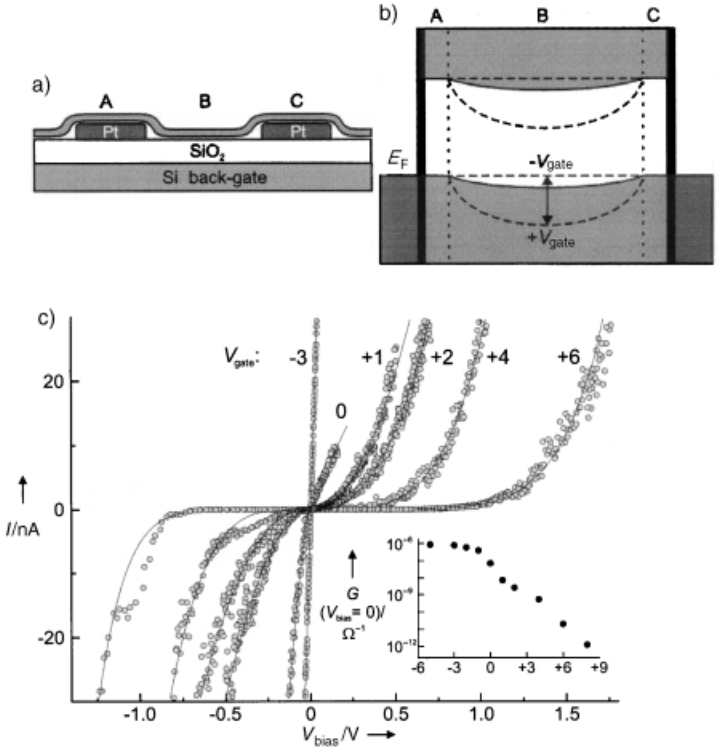

Figure 21. Nanotube field-effect transistor (TUBEFET). a) Schematic of device configuration, b) band diagram for device; the nanotube Fermi energy (E_F) is pinned at the E_F of the metal electrodes, c) I/V curves at varying V_{gate} for the device ($T = 300$ K). Inset: dependence of conductance G at $V_{bias} = 0$ with V_{gate}. Reproduced with permission from ref. [86].

applied gate biases (V_{gate}). The resulting I/V curves are shown in Figure 21c. At $V_{gate} = 0$, the I/V curve showed deviation from linearity, which indicates that this is a semiconducting nanotube. At positive values of V_{gate}, the device displayed a widening gap as V_{gate} was increased. At negative values of V_{gate}, the I/V curve showed ohmic behavior corresponding to a resistance of approximately 1 MΩ. This behavior is similar to that observed in metallic nanotubes in a similar configuration, and thus is likely to be a result of contact resistance between the nanotube and the electrodes. The inset in Figure 21c shows the change in conductance G of the device at $V_{bias} = 0$ as the V_{gate} was varied. The value of G decreased by six orders of magnitude (from 10^{-6} to $10^{-12}\,\Omega^{-1}$) as V_{gate} was made more positive. The energy diagram in Figure 21b offers an explanation for this behavior. The work function for the carbon nanotube (4.5 eV) is lower than that of the Pt electrodes (5.7 eV), but the contact between the two Pt electrodes pins the potential at the ends of the nanotube to the Fermi-level of the electrode. Thus, the valence band in the central portion of the nanotube (in contact with the SiO_2 layer, Figure 21a section B) is predicted to bend to meet the Fermi level of the electrodes. The reduced conductance at $V_{bias} = 0$ and $V_{gate} > 0$ (Figure 21b, section B) is thus a result of hole depletion, which leads to a more insulating state. At $V_{gate} < 0$, hole accumulation in section B of Figure 21b gives rise to enhanced conductance, and an ohmic (i.e., metallic) I/V curve.

The gain of the TUBEFET was low. A shift in V_{gate} from $+4$ V to $+6$ V resulted in V_{bias} shift of only around 0.7 V (Figure 21c), with a gain of approximately 0.35. Also, the frequency of operation was only about 100 GHz. A number of ways were suggested to improve these characteristics. By reducing the thickness of the SiO_2 layer from 300 nm to 5 nm and by decreasing the contact resistance to the nanotube, a theoretical operating frequency of 10 THz and a gain of approximately 3.5 were predicted.

Transistor devices based on nanosized junctions have been fabricated and display staircase I/V profiles because of a blockage of additional current flow until some threshold voltage is reached (Coulomb blockade). The threshold voltage depends on the size and nature of the particle in the semiconductor junction and varies with the junction resistance and capacitance. A Coulomb staircase profile is a special case of Coulomb blockade. When a nanostructure is small enough, the transfer of one electron onto it blocks the flow of further electrons by electrostatic repulsion. To overcome the repulsion, the voltage must be increased, until two electrons at a time can tunnel onto and off of the nanostructure. This cycle is repeated for greater numbers of electrons, and results in a step shaped I/V curve. These behaviors are useful for controlling switching behavior in very small devices, with very small currents, in very specific ways.

Sato and co-workers[87] measured the I/V properties of a single-electron transistor (SET) fabricated from a chain of colloidal gold particles with nominally 10 nm diameters. A schematic of the experimental setup is shown in Figure 22. Source, drain, and gate electrodes composed of 20 nm of Au on 5 nm of Cr were patterned on a SiO_2 surface by using electron-beam lithography. Citrate-modified Au particles, were deposited onto the surface, whereupon the citrate

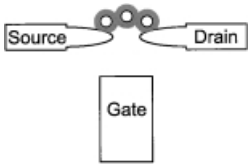

Figure 22. Schematic of an in-plane single-electron transistor. Approximately 30 nm separates the source, drain, and gate electrodes.

capping was exchanged for 1,6-hexanedithiol. A second deposition of Au particles led to the formation of short, isolated chains of Au particles on the surface. *I*/*V* measurements were carried out on samples in which the source and drain electrodes were found to be bridged by one of these chains.

I/*V* curves collected at 300, 77, and 4.2 K are shown in Figure 23 a. At 300 K, any electrons in the system have enough thermal energy to overcome any electrostatic repulsion from the particles, and tunneling onto and off of the particles is

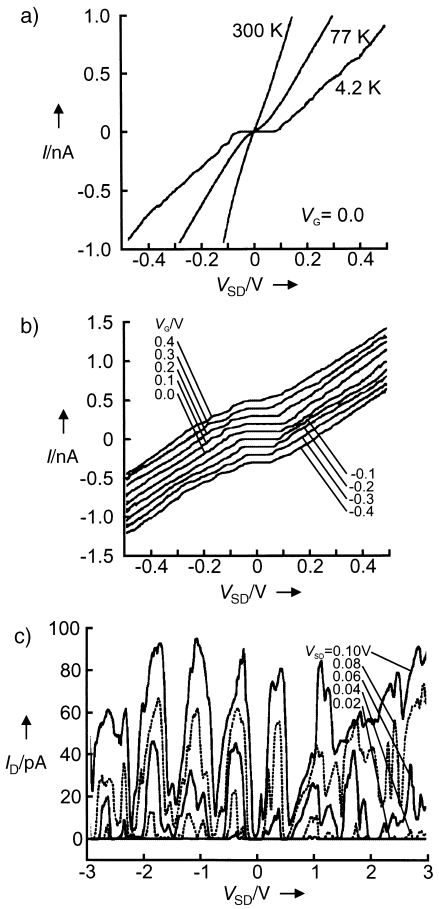

Figure 23. a) Plot of *I*/*V* curves collected between a source and drain electrode (shown in Figure 22) connected by a chain of three Au colloidal particles. V_{SD} = source – drain current. The curves were collected at the temperatures indicated, with $V_{gate} = 0$. b) Plot of *I*/*V* curves for various V_{gate} values against V_{SD}. The curves are offset from each other for clarity. c) Plot of conductance (I/V_{gate}) at various V_{SD} values. Reproduced with permission from ref. [87].

unhindered, which gives a linear *I*/*V* curve. At 4.2 K, the thermal energy of electrons in the system is much lower, and electrostatic repulsion has an effect, which gives rise to the Coulomb staircase. Figure 23 b, measured at 4.2 K, shows the variation in the *I*/*V* curve as V_{gate} is varied. The most obvious feature here is the narrowing of the Coulomb blockade as the magnitude of V_{gate} increases. Figure 23 c shows that periodic oscillations in the conductance (conductance = I/V_{gate}) become more pronounced at higher source – drain bias. Based on comparison with computational results for the system, single-electron tunneling across a four-junction system was proposed.

Andres et al. have shown Coulomb-staircase behavior at room temperature in a system composed of an Au nanoparticle (ca. 1.3 nm) bound to an Au substrate by α,ω-xylyldithiol (Figure 24).[88, 89] Previously, this behavior, characteristic of single-electron transfer events, had only been

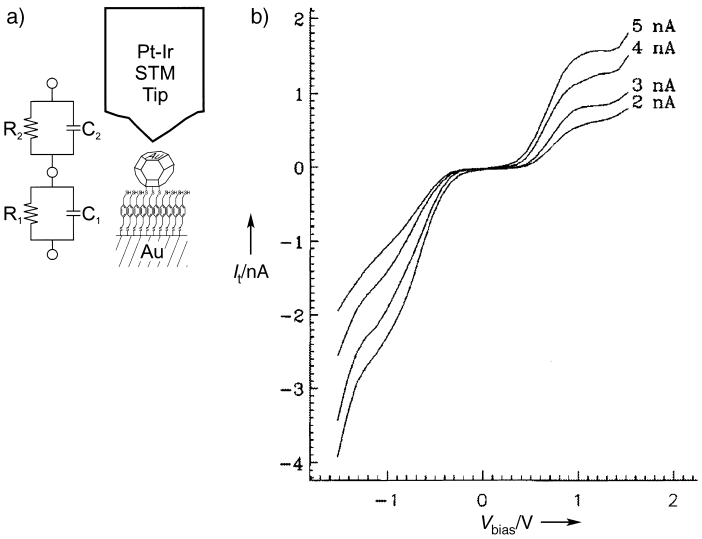

Figure 24. a) Schematic of self-assembled nanostructure, composed of xylyldithiol on an Au(111) substrate, and the circuit diagram that describes the system. b) Plot of *I*/*V* curves collected at varied setpoint currents; I_t = tunnel current. Reproduced with permission from ref. [89].

observed at very low temperatures. Fitting these *I*/*V* curves to the classical Coulomb-blockade model (each junction has a capacitance and a resistance associated with it, see Figure 24 a) verified that these curves were consistent with those of a double-tunnel junction. Further, these data allowed estimation of the resistance of a single xylyldithiol molecule ($\sim 18 \pm 12$ MΩ).

Wada has proposed using three-terminal molecular systems, such as **12**, to function as molecular single-electron switches

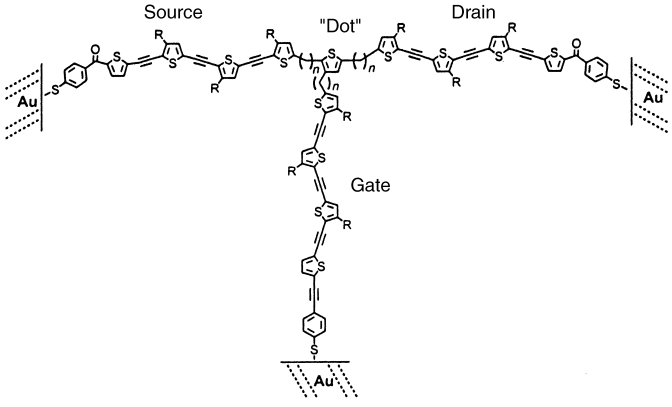

12

(MOSES).[90, 91] The source, drain, and gate are polythiophene chains or other molecular wires, and the "dot" is isolated from them by a methylene-based spacer. There still exists the very real problem of making reproducible low-resistance contacts to the "electrodes". Theoretical studies of these systems have suggested that switching speeds approaching 1 THz may be possible.

Other types of switching devices depend on the close relationship in the molecular realm between physical form and electronic structure. By changing a molecular conformation or deforming the structure of a molecule, experiments have shown that the electronic properties of the system may be modified. One of the clearest examples of this phenomenon has been the demonstration by Joachim and Gimzewski of a single-molecule electromechanical amplifier, consisting of a single C_{60} molecule between a substrate and an STM tip (Figure 25a).[92] In this experiment, a signal (V_{in}) was applied

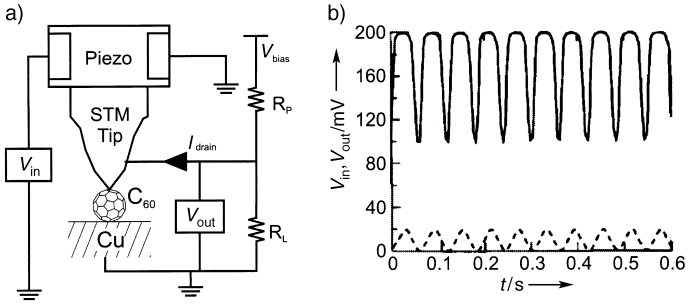

Figure 25. a) Circuit diagram of a single-molecule electromechanical amplifier based on the interaction of an STM tip with a C_{60} molecule. b) Plot of V_{in} (----) applied to piezoelectric tube and resulting V_{out} (——). Permission from ref. [92].

to the piezoelectric tube that controls the z positioning of the STM tip. This induced a distortion in the piezoelectric material, causing the STM tip to press down on the C_{60} molecule and distort it. Theoretical studies of C_{60} indicate that as it is distorted, the HOMO and LUMO are shifted and broadened,[93] which leads to a greater conductance through the molecule. The conductance of the junction was shown to increase by two orders of magnitude upon distortion. This effect is the source of the amplification in the system. In Figure 25b, the dashed sinusoidal line is V_{in}, and has a magnitude of 20 mV. The solid line is the measured output voltage (V_{out}), which shows a magnitude of 100 mV, and thus shows a gain of 5. It was suggested that the inherent limit of operational speed in this system is the first vibrational mode of C_{60} of approximately 14.7 THz. Since reporting these results, Joachim and Gimzewski have also proposed a memory device using four nano-electromechanical transistors.[14] While such a device is not terribly useful in such a configuration, the fact that a single molecule can provide a substantial gain is important for future developments in this field.

Further work showing the close relationship of conformation and electronic structure in molecules has been undertaken by Moresco et al.[94] Low-temperature STM (LT-STM) was utilized to study a substituted metalloporphyrin **13** on a Cu(211) surface. At 15 K, **13** was found to lie on the Cu(211)

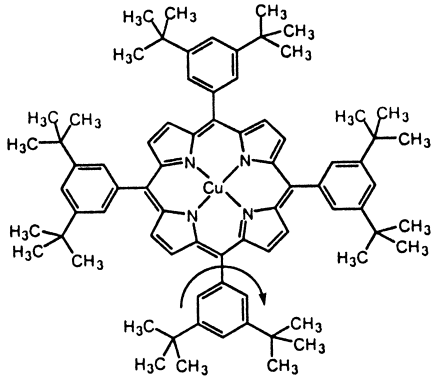

13

surface with the metalloporphyrin plane parallel to the surface. The molecule could be moved on the surface in a controllable way with the STM tip. In addition, the phenyl-*t*-butyl arms of the molecule could be oriented in two conformations (assigned from a combination of experimentation and computation)—one in which the plane of the phenyl group is about 10° from being parallel to the surface, the other in which the plane of the phenyl group is rotated at about 55° to the surface. The two conformations could be differentiated by STM (Figure 26a, b). It was also observed

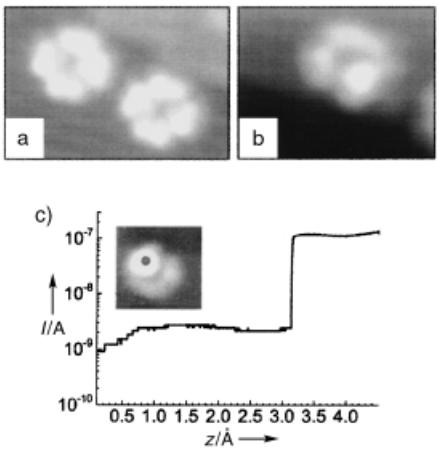

Figure 26. Low-temperature STM images of **13** on Cu(211) showing a) all *t*Bu-phenyl arms in the OFF position (nearly flat on surface), b) one arm (brighter point) in ON position (oriented 55° out of the plane of the porphyrin), and c) Plot of current on turning the ON arm OFF—the tip is moved from $z = 7.5$ Å towards surface. The dot on the inset picture indicates the tip position over the ON arm. Reproduced with permission from ref. [94].

that a lateral or vertical motion of the STM tip could induce the arm to change orientation. Further, $I(z)$ measurements (that is, variation in current as the tip was raised or lowered, with STM feedback disabled) indicated that the two different configurations have different conductances. When the STM tip was moved towards an arm in the ON position, initially the conductance was higher (indicated by current of $\approx$100 nA), until at approximately 3.0 Å, the arm had been tilted into the OFF position and current dropped by two orders of magnitude (Figure 26c).

Perhaps the smallest switching device possible would consist of an atomic relay—a single atom that can controllably be positioned in a gap and provide a clear indication of whether the switch is OFF or ON. This device would most easily operate by measuring a difference in conductance or measuring a current flow. Wada and co-workers proposed such a device with dimensions of less than 10 nm and theoretical switching speeds of 1 THz.[95] The proposal is ambitious, but out of reach with current technologies. Even so, within very strict limits based on material, a wire composed of single atoms should be able to conduct a charge from one end to the other. With this in mind, a simple atomic relay transistor can be imagined (Figure 27). In the ON state, the atom wire would carry charge through the switching atom. To turn the switch OFF, a voltage would be applied to the switching gate, and the switching atom would be shifted out of place, leaving a gap. This effectively would break the wire and stop charge transfer. To return to the ON state, a reset gate is necessary.

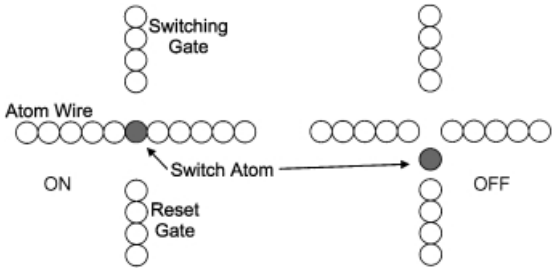

Figure 27. Proposal for an atomic relay transistor.

Clearly, such a system is not trivial to build, nor is it even obvious that the materials exist to make the device. After all, the atom wire must remain stuck to the substrate while transferring charge and must not short out to the substrate. The atom switch has to be able to shift reversibly into and out of the wire, rather than finding an energetically favorable position in the wire. The switching and reset gates must also be insulated from the atom wire, and the switching atom. Other considerations exist as well, and suggest that this is not a device that is likely to be implemented in the near future.

Even so, single-atom switching behavior has been observed. Eigler et al.[96] used the STM to reproducibly pick up and deposit a single Xe atom on a surface. At 4 K, the STM tip (composed of polycrystalline W) was used to slide a Xe atom to a kink in the Ni(110) surface. The Xe atom could be reproducibly imaged there. By applying a +800 mV pulse to the tip, the Xe atom could be made to jump onto the tip. Application of a −800 mV pulse to the tip caused the Xe atom to reattach itself to the kink. At −20 mV, with the Xe atom on the tip, a tip current of 90 nA was observed. When the Xe atom was on the surface, the current in the naked tip reduced to 15 nA. The Xe atom could be switched back and forth reproducibly by the application of the appropriate voltage pulses. To date several examples have been presented in which a probe microscope tip was used to initiate and probe switching behaviors. It is not clear if such feedback-based junctions could be viable devices (certainly there is doubt as to whether they could form viable, integrated devices). However, the probe microscope has opened up these opportunities to explicate molecular properties directly relevant to switching.

Other properties have also been used to control switching behaviors. Stoddart, Kaifer, and co-workers[97] constructed a molecular shuttle that could be switched electrostatically from one state to another. The rotaxane (Figure 28) consisted of a

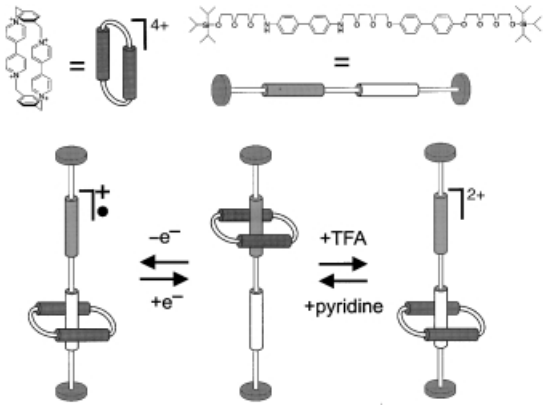

Figure 28. Representation of the construction and function of a molecular shuttle.

molecular "rod" with two "docking stations" (benzidine and benzophenol, gray and white rod segments in Figure 28, respectively), onto which was threaded a "bead" (tetracationic cyclophane). The bead was unable to dissociate from the rod because of the presence of two bulky stopper groups (tri-isopropanylsilanyl) at the ends of the rod. At room temperature, the bead traversed the length of the rod at very high rates (frequencies near 100 MHz), and there was no apparent selectivity of position on one station or the other. However, at 229 K, it was determined (by 2D NMR) that the bead exhibited 84 % occupancy at the benzidine station.

Upon addition of trifluoroacetic acid (TFA—a proton source), the bead shifted, nearly quantitatively, to the biphenol station. Neutralizing the TFA with pyridine shifted the bead back to the benzidine station. Presumably, the positive charge on the protonated benzidine repelled the cationic bead. Similarly, oxidation of the benzidine station to the radical cation shifted the bead to the benzophenol, and reduction returned it back to the benzidine. Again, this behavior is likely to be a result of electrostatic repulsion between the bead and the charged benzidine. This example, while admittedly unlikely to serve as a switch as-is, illustrates further the possibilities for controlling switching behavior in molecular devices.

The family of molecules known as rotaxanes has also been indicated as having possible utility as logical devices. A good example of this is the work by Balzani, Stoddart and co-workers[98] in which a molecular system exhibits behavior consistent with an XOR gate (Figure 29). The two starting molecules, **14** (π-electron accepting 2,7-dibenzyldiazapyrenium dication) and **15** (a crown ether containing two π-electron-

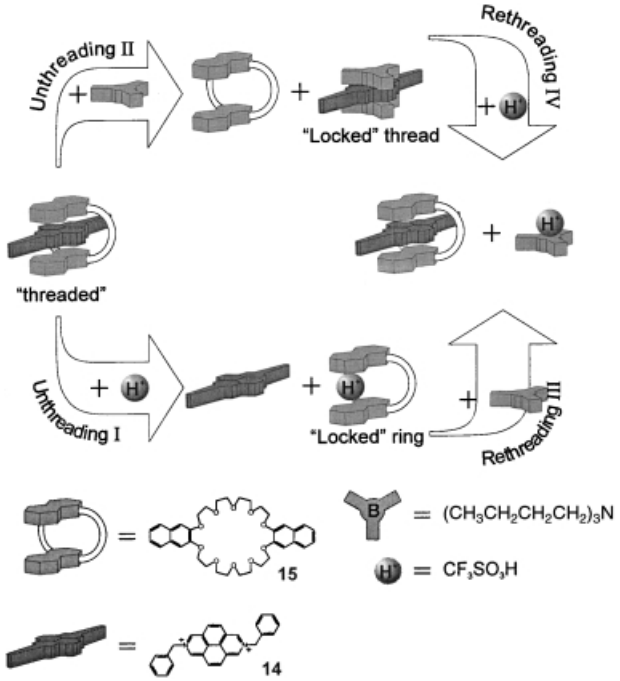

Figure 29. Schematic representation of pseudorotaxane-based logic operation.

donating 2,3-dioxynaphthalenes) form a charge-transfer complex. Separately, each of the molecules were observed to fluoresce strongly ($\lambda_{max} = 432$ and 343 nm for **14** and **15**, respectively), but upon forming the CT-complex, the fluorescence was extinguished. Adding trifluoromethanesulfonic acid ("H^+" in Figure 29) in stoichiometric amounts protonated the crown ether, largely dissociating the CT-complex ("unthreading I", in Figure 29). This action recovered the emission from $\mathbf{15} \cdot H^+$ (nearly the same as the unprotonated crown ether), as well as the emission from **14**. Adding tributylamine ("B" in Figure 29) in equivalent amount to H^+ from previous step ("rethreading III") released **15** and allowed the CT complex between **14** and **15** to reform, quenching their emission bands. In a similar fashion, adding B to the CT-complex of **14** and **15** broke up the complex ("unthreading II"), to form a $\mathbf{14} \cdot B_2$ complex. This action recovered the strong emission from **15**. In addition to a new broad emission from the $\mathbf{14} \cdot B_2$ at 670 nm was observed. Adding H^+ to this adduct released **14**, which rethreaded with **15** ("rethreading IV"), once again quenching the fluorescence of the separate components.

Examination of this sequence reveals a pattern: Whenever the two components **14** and **15** are in the presence of either B or H^+, there was a strong fluorescence at 343 nm. If both B or H^+, were present, there was no fluorescence. If neither was present, there was no fluorescence. If the fluorescence is taken as an indicator of truth, and B and H^+ are taken as inputs, then the system has the same behavior as an XOR gate (see Table 2).

Drawing comparisons between chemical systems and logic operations or switching behavior must be undertaken carefully. The purpose here is to illustrate the very great flexibility of purpose to be found when dealing with molecular systems,

Table 2. XOR Truth Table.

Input X	Input Y	Output
false	false	false
false	true	true
true	false	true
true	true	false

not to suggest that either of these systems might somehow be integrated into a "wet" computer.

Using another, catenane-based system, anchored with amphiphilic phospholipid counterions, and sandwiched between an n-type polycrystalline Si electrode and a Ti/Al top electrode, a device exhibiting hysteretic (bistable) current/voltage characteristics was demonstrated (Figure 30).[99] This switch could be opened at +2 V, closed at −2 V, and read between 0.1 and 0.3 V. Using this hysteretic behavior, many read–write cycles were demonstrated. The demonstration of hysteretic behavior here is particularly notable—this basic illustration convincingly establishes that the device can retain its state after the application of the read voltage.

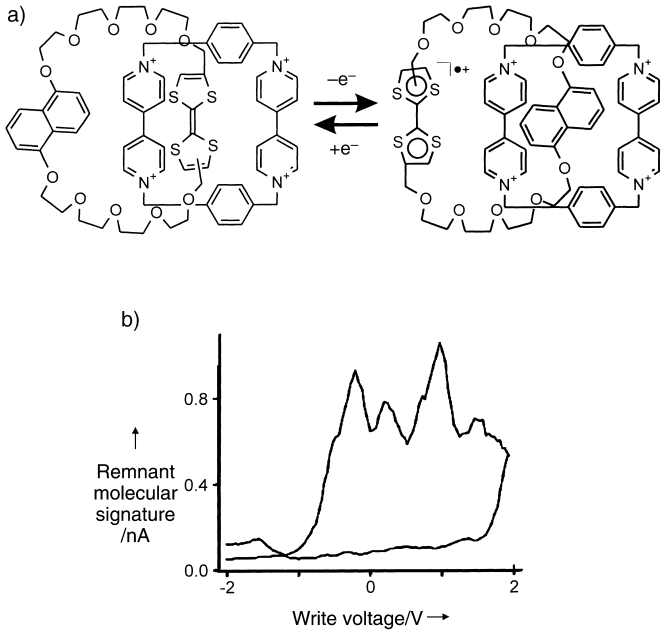

Figure 30. a) Two conformers of an electroactive, bistable molecule. b) The remnant molecular signature of a catenane-based device, measured by varying the write voltage in 40-mV steps and by reading the device at −0.2 V. Reproduced with permission from ref. [99].

2.5. Nonlinear Behaviors—Negative Differential Resistance

A negative differential resistance (NDR) is characterized by a discontinuity in the monotonic increase of current as the voltage is increased. That is, as voltage goes up, current plateaus, or in the most interesting cases, decreases before eventually rising again. This behavior is found in Esaki[100] and resonant tunneling diodes[101] for which several applications have been proposed. Several of these devices can be combined to give *I*/*V* curves with multiple peaks—this

behavior has been proposed to lead to multi-state memory and logic devices. From the standpoint of molecular-device construction, wiring a molecule to two-terminals appears technically more feasible than wiring to three-terminals (transistors are three terminal electronic devices). Thus, this avenue of molecular electronics has been pursued extensively. However, it is not clear that such devices can be integrated as they do not, by themselves, offer the opportunity to introduce gain into a circuit. Thus, two-terminal devices represent a tradeoff between what is currently feasible and potential real utility in circuit construction. At this time, the "jury is still out" with respect to two-terminal, molecular-based electronics.

Reed and Tour et al. reported the clearest example of molecule-based NDR to date.[102] Molecule **16** was sandwiched between two metal contacts. At 60 K, this assembly was found to display a very strong NDR with a peak-to-valley ratio (PVR) of 1030:1 and this value decreased as temperature increased (Figure 31). Control molecules (having no nitro or amine moieties) showed no NDR. The NDR was proposed to arise as a consequence of a two-step reduction: an initial one-electron reduction of the molecule provides charge carriers, and allows current flow. Current flow continues until the second reduction potential is reached, and the molecule is reduced to the dianion. Recently, Reed and Tour et al. have examined another molecule, similar to **16**, but without the amine functionality, which shows weak NDR at room temperature.[103] The proposed mechanism has been investigated computationally, and the results have proven somewhat contentious. Seminario and co-workers[104] tested the proposed mechanism with ab initio techniques, and found that, as observed, the current flow should be able to travel through the molecule only when it was reduced, as the LUMO at this point extended across the whole length of the molecule. Birge et al., however, have suggested that an oxidation occurs, and conduction occurs resonantly through the HOMO.[105]

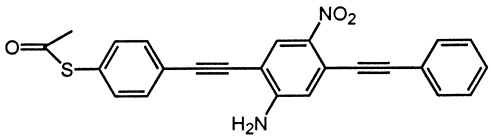

16

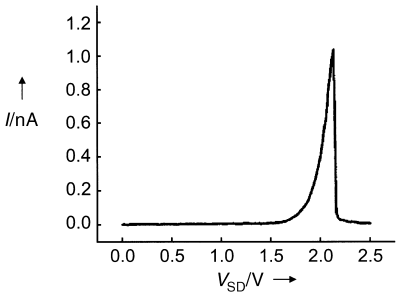

Figure 31. Graph of an *I*/*V* curve of **16** collected at 60 K. Reproduced with permission from ref. [102].

In another notable example of molecular NDR,[106] the *I*/*V* properties of **17** were studied with tunneling spectroscopy.

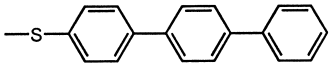

17

Figure 32 shows the observed *I*/*V* curve, with NDR at both negative and positive potentials. To explain this result a different mechanism was proposed. In this instance, the NDR was thought to arise not from any sort of oxidation or reduction, but rather a resonance between the tip and the molecule–substrate complex. In the case of a very sharp STM tip, it was suggested that the tip presents narrow features in the density-of-states (DOS) profile. The molecule, with discrete molecular levels, also presents narrow features in its DOS profile. Since the molecule is bound to a substrate through a relatively strong thiol–gold bond, the molecular DOS tends to float with the E_F of the substrate. As a bias is applied between the substrate and the tip, the molecular levels shift in one direction, while the tip DOS shifts the other. If the narrow features in the two DOS should cross one another, NDR should occur. Very recently, Brèdas et al. have presented some computational data to further illustrate the necessity of a reduced density of states in the contact for NDR behavior to be displayed in a molecular system.[107]

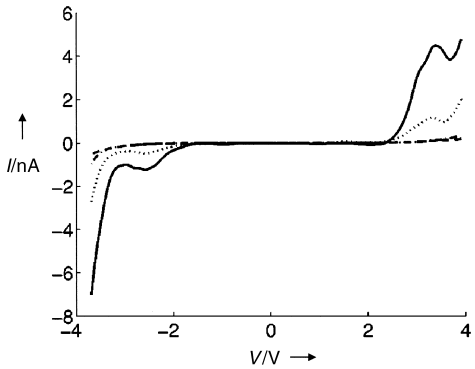

Figure 32. The *I*/*V* curve collected by STM over a monolayer of **17**. Setpoint bias was −5.0 V, and the tunneling current was varied from 3.05 to 30.5 nA. Reproduced with permission from ref. [106].

We recently observed NDR in *I*/*V* curves collected with an STM tip over a ferrocene-terminated SAM composed of **18**.[108] Figure 33a shows representative *I*/*V* curves collected over a region composed of **18** and dodecanethiol SAM. Those

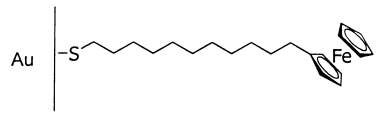

18

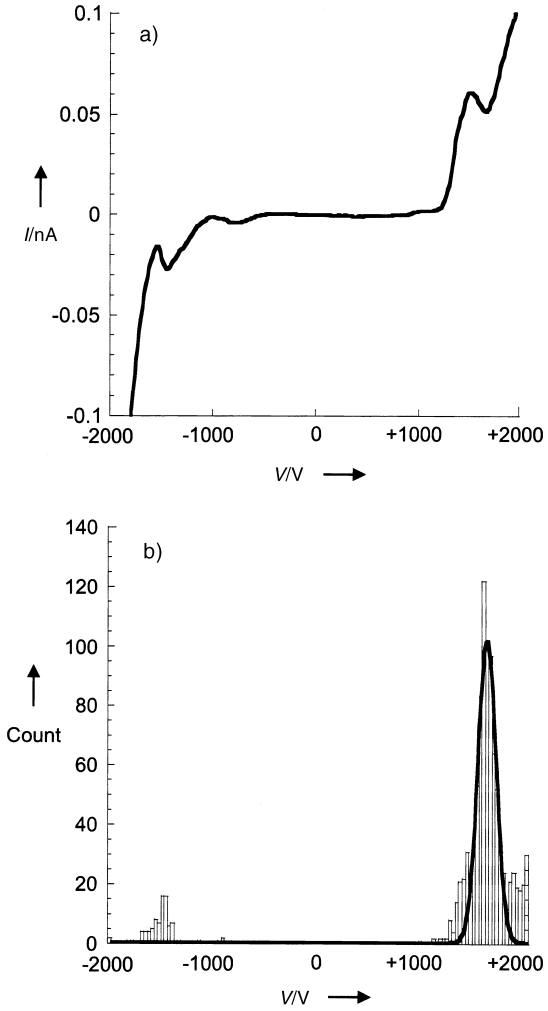

Figure 33. a) A typical *I/V* curve collected from a SAM of **18** under dodecane. b) Histogram representing the position of the NDR in a SAM of **18** under dodecane. Reproduced with permission from ref. [108].

curves from the **18** region show a nonlinearity characteristic of NDR. A histogram of the peak position from many different measurements is shown in Figure 33 b. It was suggested that the accessible redox states in the ferrocene headgroup of **18** allow resonant tunneling through the molecule, giving rise to the NDR. This observation is significant in that it suggests that the position of NDR should be related to redox potential, and may offer a route to tunable NDR. Further work to characterize the generality of the behavior in other systems is underway.

Berg et al.[109] examined the published reports of molecular and III-V semiconductor resonant tunneling devices (RTDs), to determine if they met the requirements set forth by the International Technology Roadmap for Semiconductors. The roadmap goals for 2008 regarding RTD usage as a Dynamic-RAM-refresh were used for the criteria. The published *I/V* curves for a number of systems, which included **16**, were used to determine the operating parameters for each RTD. The results are presented in Figure 34 where "Mol60 K" represents the results based on **16**. The area occupied on the plot determines the effectiveness of an RTD. The larger the plotted area, then the larger the acceptable range of supply

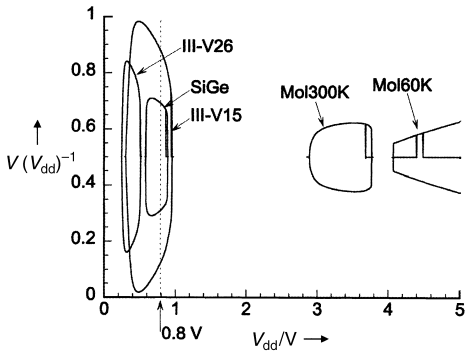

Figure 34. Plot of stable voltages for recently published RTDs as a function of supply voltage; V_{dd} = supply voltage. Reproduced with permission from ref. [109].

voltages for the device and the larger the difference in it's ON and OFF states. Berg and co-workers concluded that the currently available molecular and semiconductor species do not meet the requirements for a useful RTD, and suggest a number of goals. They suggest that while good PVRs are important, it is more important to have a low valley current, and that the "simplest" way to achieve this is to use fewer, or even single, molecules as operative devices. In addition, future molecules will have to be designed to show a much lower "turn-on" voltage.

3. Closing Thoughts

There is great promise to molecular electronics—electronics that are smaller, faster, more efficient, and potentially more flexible (in multiple ways) than conventional electronics. Clearly, some viable, fundamental demonstrations have been made of molecular-scale electronic-device behaviors. This review is entitled a "genesis", however, as the fundamental understanding of these behaviors is still lacking. More extensive characterization to deduce the molecular origin of these behaviors is in order. All of this must happen in a highly collaborative, interdisciplinary arena and a broad view will be required from all involved. Chemists, physicists, materials scientists, and electrical and chemical engineers must work together to understand the many facets of the research problems that are being uncovered as the field grows. The excitement of new demonstration coupled with the simpler, more elegant quest to understand makes molecular electronics an exciting and potentially very lucrative field.[115]

We thank the National Science Foundation (Grants CHE-9900072 and DMR-9600138) and the Office of Naval Research for support of this work. We also thank Stefan Kraemer and Ryan Fuier for critical reading of this work.

Received: December 18, 2001 [A 507]

[1] J. S. C. Kilby, *ChemPhysChem* **2001**, *2*, 482.
[2] G. E. Moore, *Electronics* **1965**, *38*, 114.
[3] G. E. Moore in *Digest of the 1975 International Electron Devices Meeting*, IEEE, New York, **1975**, p. 1113.

[4] *The International Technology Roadmap for Semiconductors—2000 Update* (http://public.itrs.net/).
[5] K. Deguchi, T. Haga, *C. R. Acad. Sci. Ser. IV:Phys. Astrophys.* **2000**, *1*, 829.
[6] G. F. Cardinale, C. C. Henderson, J. E. M. Goldsmith, P. J. S. Mangat, J. Cobb, S. D. Hector, *J. Vac. Sci. Technol. B* **1999**, *17*, 2970.
[7] D. A. Muller, T. Sorsch, S. Moccio, F. H. Baumann, K. Evans-Lutterodt, G. Timp, *Nature* **1999**, *399*, 758.
[8] G. Ghibaudo, R. Clerc, E. Vincent, S. Bruyere, J. L. Autran, *C. R. Acad. Sci. Ser. IV*: *Phys. Astrophys.* **2000**, *1*, 911.
[9] S. Chiras, D. R. Clarke, *J. Appl. Phys.* **2000**, *88*, 6302.
[10] D. Edelstein, J. Heidenreich, R. Goldblatt, W. Cote, C. Uzoh, N. Lustig, P. Roper, T. McDevitt, W. Motsiff, A. Simon, J. Dukovic, R. Wachnik, H. Rathore, R. Schulz, L. Su, S. Luce, J. Slattery, *Tech. Dig. Int. Electron Devices Meet.* **1997**, 773.
[11] D. J. Kim, Y. B. Jung, M. B. Lee, Y. H. Lee, J. H. Lee, *Thin Solid Films* **2000**, *372*, 276.
[12] S. J. Martin, J. P. Godschalx, M. E. Mills, E. O. Shaffer, P. H. Townsend, *Adv. Mater.* **2000**, *12*, 1769.
[13] Review: D. GoldhaberGordon, M. S. Montemerlo, J. C. Love, G. J. Opiteck, *Proc. IEEE* **1997**, *85*, 521.
[14] Review: C. Joachim, J. K. Gimzewski, A. Aviram, *Nature* **2000**, *408*, 541.
[15] Richard Feynman gave this talk entitled "There's Plenty of Room at the Bottom" on December 29th, 1959, at the annual meeting of the American Physical Society at the California Institute of Technology.
[16] A similar definition was used recently, see: http://www.darpa.mil/DSO/solicitations/00/Baa00–39/cbd.htm and http://www.darpa.mil/MTO/mole/.
[17] T. A. Jung, R. R. Schlittler, J. K. Gimzewski, H. Tang, C. Joachim, *Science* **1996**, *271*, 181.
[18] A. Aviram, M. A. Ratner, *Chem. Phys. Lett.* **1974**, *29*, 277.
[19] A. Aviram, C. Joachim, M. Pomerantz, *Chem. Phys. Lett.* **1988**, *146*, 490.
[20] A. Aviram, *Chem. Phys. Lett.* **1989**, *162*, 416.
[21] M. Pomerantz, A. Aviram, R. A. McCorkle, L. Li, A. G. Schrott, *Science* **1992**, *255*, 1115.
[22] A. S. Martin, J. R. Sambles, G. J. Ashwell, *Phys. Rev. Lett.* **1993**, *70*, 218.
[23] R. M. Metzger, B. Chen, U. Höpfner, M. V. Lakshmikantham, D. Vuillaume, T. Kawai, X. L. Wu, H. Tachibana, T. V. Hughes, H. Sakurai, J. W. Baldwin, C. Hosch, M. P. Cava, L. Brehmer, G. J. Ashwell, *J. Am. Chem. Soc.* **1997**, *119*, 10455.
[24] A. Broo, M. C. Zerner, *Chem. Phys.* **1995**, *196*, 423.
[25] A. Aviram, *J. Am. Chem. Soc.* **1988**, *110*, 5687.
[26] K. Müllen, G. Wegner, *Electronic Materials: The Oligomer Approach*, Wiley-VCH, Weinheim, **1998**.
[27] R. Dembinski, T. Bartik, B. Bartik, M. Jaeger, J. A. Gladysz, *J. Am. Chem. Soc.* **2000**, *122*, 810.
[28] M. J. Crossley, P. L. Burn, *J. Chem. Soc. Chem. Commun.* **1991**, 1569.
[29] M. J. Crossley, P. L. Burn, *J. Chem. Soc. Chem. Commun.* **1987**, 39.
[30] J. R. Reimers, L. E. Hall, M. J. Crossley, N. S. Hush, *J. Phys. Chem. A* **1999**, *103*, 4385.
[31] D. L. Pearson, J. M. Tour, *J. Org. Chem.* **1997**, *62*, 1376.
[32] L. Jones, J. S. Schumm, J. M. Tour, *J. Org. Chem.* **1997**, *62*, 1388.
[33] M. T. Cygan, T. D. Dunbar, J. J. Arnold, L. A. Bumm, N. F. Shedlock, T. P. Burgin, L. Jones II, D. L. Allara, J. M. Tour, P. S. Weiss, *J. Am. Chem. Soc.* **1998**, *120*, 2721.
[34] L. A. Bumm, J. J. Arnold, M. T. Cygan, T. D. Dunbar, T. P. Burgin, L. Jones, D. L. Allara, J. M. Tour, P. S. Weiss, *Science* **1996**, *271*, 1705.
[35] M. S. Doescher, J. M. Tour, A. M. Rawlett, M. L. Myrick, *J. Phys. Chem. B* **2001**, *105*, 105.
[36] A. Ulman, *An Introduction to Ultrathin Organic Films from Langmuir-Blodgett to Self-Assembly*, Academic Press, New York, **1991**, p. 278.
[37] V. Balzani, *Electron Transfer in Chemistry*, Wiley-VCH, Weinheim, **2001**.
[38] K. Slowinski, H. K. Y. Fong, M. Majda, *J. Am. Chem. Soc.* **1999**, *121*, 7257.
[39] K. Slowinski, R. V. Chamberlain, C. J. Miller, M. Majda, *J. Am. Chem. Soc.* **1997**, *119*, 11910.
[40] R. E. Holmlin, R. Haag, M. L. Chabinyc, R. F. Ismagilov, A. E. Cohen, A. Terfort, M. A. Rampi, G. M. Whitesides, *J. Am. Chem. Soc.* **2001**, *123*, 5075.
[41] M. A. Rampi, O. J. A. Schueller, G. M. Whitesides, *Appl. Phys. Lett.* **1998**, *72*, 1781.
[42] R. E. Holmlin, R. F. Ismagilov, R. Haag, V. Mujica, M. A. Ratner, M. A. Rampi, G. M. Whitesides, *Angew. Chem.* **2001**, *113*, 2378; *Angew. Chem. Int. Ed.* **2001**, *40*, 2316.
[43] D. J. Wold, C. D. Frisbie, *J. Am. Chem. Soc.* **2000**, *122*, 2970.
[44] W. B. Davis, W. A. Svec, M. A. Ratner, M. R. Wasielewski, *Nature* **1998**, *396*, 60.
[45] S. N. Yaliraki, M. Kemp, M. A. Ratner, *J. Am. Chem. Soc.* **1999**, *121*, 3428.
[46] H. D. Sikes, J. F. Smalley, S. P. Dudek, A. R. Cook, M. D. Newton, C. E. D. Chidsey, S. W. Feldberg, *Science* **2001**, *291*, 1519.
[47] D. E. Khoshtariya, T. D. Dolidze, L. D. Zusman, D. H. Waldeck, *J. Phys. Chem. A* **2001**, *105*, 1818.
[48] W. B. Davis, M. A. Ratner, M. R. Wasielewski, *J. Am. Chem. Soc.* **2001**, *123*, 7877.
[49] D. Segal, A. Nitzan, W. B. Davis, M. R. Wasielewski, M. A. Ratner, *J. Phys. Chem. B* **2000**, *104*, 3817.
[50] B. Giese, *Acc. Chem. Res.* **2000**, *33*, 631.
[51] M. W. Grinstaff, *Angew. Chem.* **1999**, *111*, 3845; *Angew. Chem. Int. Ed.* **1999**, *38*, 3629.
[52] Y. A. Berlin, A. L. Burin, M. A. Ratner, *J. Am. Chem. Soc.* **2001**, *123*, 260.
[53] Y. A. Berlin, A. L. Burin, M. A. Ratner, *J. Phys. Chem. A* **2000**, *104*, 443.
[54] F. D. Lewis, X. Y. Liu, J. Q. Liu, S. E. Miller, R. T. Hayes, M. R. Wasielewski, *Nature* **2000**, *406*, 51.
[55] A. Thess, R. Lee, P. Nikolaev, H. J. Dai, P. Petit, J. Robert, C. H. Xu, Y. H. Lee, S. G. Kim, A. G. Rinzler, D. T. Colbert, G. E. Scuseria, D. Tomanek, J. E. Fischer, R. E. Smalley, *Science* **1996**, *273*, 483.
[56] C. Journet, W. K. Maser, P. Bernier, A. Loiseau, M. L. de la Chapelle, S. Lefrant, P. Deniard, R. Lee, J. E. Fischer, *Nature* **1997**, *388*, 756.
[57] M. S. Dresselhaus, G. Dresselhaus, P. C. Eklund, *Science of Fullerenes and Carbon Nanotubes*, Academic Press, San Diego, **1996**.
[58] M. S. Dresselhaus, G. Dresselhaus, P. Avouris, *Carbon Nanotubes: Synthesis, Structure, Properties, and Applications*, Springer, Berlin, **2001**.
[59] J. W. G. Wildoer, L. C. Venema, A. G. Rinzler, R. E. Smalley, C. Dekker, *Nature* **1998**, *391*, 59.
[60] T. W. Odom, J. L. Huang, P. Kim, C. M. Lieber, *Nature* **1998**, *391*, 62.
[61] A. Bachtold, M. Henny, C. Tarrier, C. Strunk, C. Schonenberger, J. P. Salvetat, J. M. Bonard, L. Forro, *Appl. Phys. Lett.* **1998**, *73*, 274.
[62] P. J. de Pablo, C. Gómez-Navarro, A. Gil, J. Colchero, M. T. Martinez, A. M. Benito, W. K. Maser, J. Gómez-Herrero, A. M. Baró, *Appl. Phys. Lett.* **2001**, *79*, 2979.
[63] P. J. de Pablo, M. T. Martinez, J. Colchero, J. Gómez-Herrero, W. K. Maser, A. M. de Benito, E. Munoz, A. M. Baró, *Mater. Sci. Eng. C* **2001**, *15*, 149.
[64] T. Hanrath, B. A. Korgel, *J. Am. Chem. Soc.* **2002**, *124*, 1424.
[65] Y. Y. Wu, R. Fan, P. D. Yang, *Nano Lett.* **2002**, *2*, 83.
[66] Z. W. Pan, Z. R. Dai, C. Ma, Z. L. Wang, *J. Am. Chem. Soc.* **2002**, *124*, 1817.
[67] J. C. Johnson, H. Q. Yan, R. D. Schaller, L. H. Haber, R. J. Saykally, P. D. Yang, *J. Phys. Chem. B* **2001**, *105*, 11387.
[68] H. Kind, H. Q. Yan, B. Messer, M. Law, P. D. Yang, *Adv. Mater.* **2002**, *14*, 158.
[69] J. F. Wang, M. S. Gudiksen, X. F. Duan, Y. Cui, C. M. Lieber, *Science* **2001**, *293*, 1455.
[70] M. H. Huang, S. Mao, H. Feick, H. Q. Yan, Y. Y. Wu, H. Kind, E. Weber, R. Russo, P. D. Yang, *Science* **2001**, *292*, 1897.
[71] F. Favier, E. C. Walter, M. P. Zach, T. Benter, R. M. Penner, *Science* **2001**, *293*, 2227.
[72] Y. Cui, Q. Q. Wei, H. K. Park, C. M. Lieber, *Science* **2001**, *293*, 1289.
[73] Y. Cui, C. M. Lieber, *Science* **2001**, *291*, 851.
[74] X. F. Duan, Y. Huang, Y. Cui, J. F. Wang, C. M. Lieber, *Nature* **2001**, *409*, 66.
[75] Y. Huang, X. F. Duan, Y. Cui, L. J. Lauhon, K. H. Kim, C. M. Lieber, *Science* **2001**, *294*, 1313.
[76] B. Messer, J. H. Song, P. D. Yang, *J. Am. Chem. Soc.* **2000**, *122*, 10232.

[77] C. M. Lieber, *Nano Lett.* **2002**, *2*, 81.
[78] M. S. Gudiksen, L. J. Lauhon, J. Wang, D. C. Smith, C. M. Lieber, *Nature* **2002**, *415*, 617.
[79] T. Rueckes, K. Kim, E. Joselevich, G. Y. Tseng, C. L. Cheung, C. M. Lieber, *Science* **2000**, *289*, 94.
[80] Y. K. Kwon, D. Tomanek, S. Iijima, *Phys. Rev. Lett.* **1999**, *82*, 1470.
[81] G. Binnig, M. Despont, U. Drechsler, W. Häberle, M. Lutwyche, P. Vettiger, H. J. Mamin, B. W. Chui, T. W. Kenny, *Appl. Phys. Lett.* **1999**, *74*, 1329.
[82] M. I. Lutwyche, M. Despont, U. Drechsler, U. Dürig, W. Häberle, H. Rothuizen, R. Stutz, R. Widmer, G. K. Binnig, P. Vettiger, *Appl. Phys. Lett.* **2000**, *77*, 3299.
[83] P. Vettiger, M. Despont, U. Drechsler, U. Dürig, W. Häberle, M. I. Lutwyche, H. E. Rothuizen, R. Stutz, R. Widmer, G. K. Binnig, *IBM J. Res. Dev.* **2000**, *44*, 323.
[84] K. M. Roth, N. Dontha, R. B. Dabke, D. T. Gryko, C. Clausen, J. S. Lindsey, D. F. Bocian, W. G. Kuhr, *J. Vac. Sci. Technol. B* **2000**, *18*, 2359.
[85] B. L. Feringa, *Molecular Switches*, Wiley-VCH, Weinheim, **2001**.
[86] S. J. Tans, A. R. M. Verschueren, C. Dekker, *Nature* **1998**, *393*, 49.
[87] T. Sato, H. Ahmed, D. Brown, B. F. G. Johnson, *J. Appl. Phys.* **1997**, *82*, 696.
[88] R. P. Andres, T. Bein, M. Dorogi, S. Feng, J. I. Henderson, C. P. Kubiak, W. Mahoney, R. G. Osifchin, R. Reifenberger, *Science* **1996**, *272*, 1323.
[89] R. P. Andres, S. Datta, M. Dorogi, J. Gomez, J. I. Henderson, D. B. Janes, V. R. Kolagunta, C. P. Kubiak, W. Mahoney, R. F. Osifchin, R. Reifenberger, M. P. Samanta, W. Tian, *J. Vac. Sci. Technol. A* **1996**, *14*, 1178.
[90] Y. Wada, *Pure Appl. Chem.* **1999**, *71*, 2055.
[91] Y. Wada, *J. Vac. Sci. Technol. A* **1999**, *17*, 1399.
[92] C. Joachim, J. K. Gimzewski, *Chem. Phys. Lett.* **1997**, *265*, 353.
[93] C. Joachim, J. K. Gimzewski, R. R. Schlittler, C. Chavy, *Phys. Rev. Lett.* **1995**, *74*, 2102.
[94] F. Moresco, G. Meyer, K. H. Rieder, H. Tang, A. Gourdon, C. Joachim, *Phys. Rev. Lett.* **2001**, *86*, 672.
[95] Y. Wada, T. Uda, M. Lutwyche, S. Kondo, S. Heike, *J. Appl. Phys.* **1993**, *74*, 7321.
[96] D. M. Eigler, C. P. Lutz, W. E. Rudge, *Nature* **1991**, *352*, 600.
[97] R. A. Bissell, E. Cordova, A. E. Kaifer, J. F. Stoddart, *Nature* **1994**, *369*, 133.
[98] A. Credi, V. Balzani, S. J. Langford, J. F. Stoddart, *J. Am. Chem. Soc.* **1997**, *119*, 2679.
[99] C. P. Collier, G. Mattersteig, E. W. Wong, Y. Luo, K. Beverly, J. Sampaio, F. M. Raymo, J. F. Stoddart, J. R. Heath, *Science* **2000**, *289*, 1172.
[100] S. M. Sze, *Physics of Semiconductor Devices*, 2nd Ed., Wiley, New York, **1981**.
[101] R. H. Mathews, J. P. Sage, T. C. L. G. Sollner, S. D. Calawa, C.-L. Chen, L. J. Mahoney, P. A. Maki, K. M. Molvar, *Proc. IEEE* **1999**, *87*, 596.
[102] J. Chen, M. A. Reed, A. M. Rawlett, J. M. Tour, *Science* **1999**, *286*, 1550.
[103] J. Chen, W. Wang, M. A. Reed, A. M. Rawlett, D. W. Price, J. M. Tour, *Appl. Phys. Lett.* **2000**, *77*, 1224.
[104] J. M. Seminario, A. G. Zacarias, J. M. Tour, *J. Am. Chem. Soc.* **2000**, *122*, 3015.
[105] A. W. Ghosh, F. Zahid, S. Datta, R. R. Birge, *Chem. Phys.* **2002**, *281*, 225.
[106] Y. Q. Xue, S. Datta, S. Hong, R. Reifenberger, J. I. Henderson, C. P. Kubiak, *Phys. Rev. B* **1999**, *59*, R7852.
[107] Y. Karzazi, J. Cornil, J. L. Brédas, *J. Am. Chem. Soc.* **2001**, *123*, 10076.
[108] C. B. Gorman, R. L. Carroll, R. R. Fuierer, *Langmuir* **2001**, *17*, 6923.
[109] J. Berg, S. Bengtsson, P. Lundgren, *Solid-State Electron.* **2000**, *44*, 2247.
[110] S. Creager, C. J. Yu, C. Bamdad, S. O'Connor, T. MacLean, E. Lam, Y. Chong, G. T. Olsen, J. Y. Luo, M. Gozin, J. F. Kayyem, *J. Am. Chem. Soc.* **1999**, *121*, 1059.
[111] J. R. Reimers, T. X. Lu, M. J. Crossley, N. S. Hush, *Nanotechnology* **1996**, *7*, 424.
[112] C. Joachim, J. P. Launay, S. Woitellier, *Chem. Phys.* **1990**, *147*, 131.
[113] K. Weber, L. Hockett, S. Creager, *J. Phys. Chem. B* **1997**, *101*, 8286.
[114] P. G.. Collins, M. S. Arnold, P. Avouris, *Science* **2001**, *292*, 706.
[115] Since the submission of this review, two significant papers that address this issue have appeared. a) J. Park, A. N. Pasupathy, J. I. Goldsmith, C. Chang, Y. Aish, J. R. Petta, M. Rinkoski, J. P. Sethna, H. D. Abruña, P. L. McEuen, D. C. Ralph, *Nature* **2002**, *417*, 722; b) W. Liang, M. P. Shores, M. Bockrath, J. R. Long, H. Park, *Nature* **2002**, *417*, 725.